

1 Comparative analysis of liquefaction susceptibility assessment methods based on the 2 investigation on a pilot site in the greater Lisbon area

3
4 Cristiana Ferreira¹ (corresponding author), António Viana da Fonseca², Catarina Ramos³, Ana Sofia Saldanha⁴,
5 Sara Amoroso⁵, Carlos Rodrigues⁶

6
7 ¹ *CONSTRUCT-GEO. Faculty of Engineering of University of Porto, Portugal, Rua Roberto Frias, s/n 4200-465, Porto,*
8 *Portugal, email: cristiana@fe.up.pt, telephone: +351225081752. ORCID: 0000-0001-5998-6220.*

9 ² *CONSTRUCT-GEO. Faculty of Engineering of University of Porto, Portugal, Rua Roberto Frias, s/n 4200-465, Porto,*
10 *Portugal. ORCID: 0000-0002-9896-1410.*

11 ³ *CONSTRUCT-GEO. Faculty of Engineering of University of Porto, Portugal, Rua Roberto Frias, s/n 4200-465, Porto,*
12 *Portugal. ORCID: 0000-0001-6679-8121.*

13 ⁴ *Faculty of Engineering of University of Porto, Portugal, Rua Roberto Frias, s/n 4200-465, Porto, Portugal.*

14 ⁵ *University of Chieti-Pescara, Viale Pindaro, Pescara, Italy; formerly Istituto Nazionale di Geofisica e Vulcanologia,*
15 *Viale Crispi, L'Aquila, Italy. ORCID: 0000-0001-5835-079X*

16 ⁶ *Polytechnic Institute of Guarda, Av. Dr. Francisco Sá Carneiro, 50, 6300-559 Guarda Portugal. ORCID: 0000-0003-*
17 *1054-0468.*

18
19 **ABSTRACT:** In Portugal, particularly in the greater Lisbon area, there are widespread alluvial sandy deposits,
20 which need to be carefully assessed in terms of liquefaction susceptibility and risk zonation. For this purpose,
21 a pilot site has been set up, as part of the European H2020 LIQUEFACT project. An extensive database of
22 geological and geotechnical reports was collected and a comprehensive site investigation campaign was carried
23 out, including boreholes with standard penetration (SPT), piezocone penetrometer (CPTu) and seismic
24 dilatometer (SDMT) tests as well as geophysical methods, complemented by undisturbed soil sampling for
25 laboratory characterisation. The assessment of liquefaction susceptibility based on field tests was made using
26 the simplified procedure, considering the factor of safety against liquefaction (FS_{liq}), which relates the cyclic
27 resistance ratio (CRR) with the cyclic stress ratio (CSR). While the computation of the CSR is relatively
28 straightforward, the reliability of the CRR strongly depends on the adopted in situ testing technique. Alternative
29 approaches to liquefaction assessment have been proposed, based on quantitative liquefaction damage indexes,
30 namely the Liquefaction Potential Index (LPI) and Liquefaction Severity Number (LSN). In this paper, the
31 geotechnical field data is integrated in these distinct approaches to liquefaction assessment. A comparative and
32 in-depth analysis of the conventional approach is presented and the inclusion of specific information on soil
33 type, as a means to overcome the observed differences, is discussed particularly for SPT and V_s results. The
34 combination of these criteria enabled to clearly identify the most critical layers, in terms of liquefaction
35 potential and severity.

36
37 **Keywords:** Earthquake-induced liquefaction; Liquefaction potential; Site characterisation; In situ tests;
38 Lisbon earthquake

39 1. Background on liquefaction assessment methods

40
41 Different approaches to the assessment of the liquefaction potential have been proposed. The most common
42 approach is the ‘‘Simplified Procedure’’, originally proposed by Seed and Idriss (1967), which is also
43 recommended by Eurocode 8 or EC8 (CEN, 2010). According to this procedure, the factor of safety against
44 liquefaction is computed from the ratio between the cyclic resistance ratio (CRR) and the cyclic stress ratio
45 (CSR), as in Equation 1. The CRR refers to the resisting capacity of the soil to liquefy, while the CSR
46 corresponds to the design seismic action at a specific location in depth.

$$47 \quad FS_{liq} = \frac{CRR}{CSR} \quad (1)$$

48 The liquefaction analysis framework proposed by Boulanger and Idriss (2014) was adopted, which is based on
49 the simplified procedure proposed by Seed and Idriss (1967) and uses the parameters from previous works,
50 namely r_d from Idriss (1999), K_σ from Idriss and Boulanger (2008) and the implementation of the fines content
51 estimates from CPT (Idriss and Boulanger, 2008). In this approach, the resistance values from SPT and CPTu
52 are adjusted to incorporate the effect of fines content. Table 1 presents a summary of the expressions for
53 computation of the governing parameters used in this analysis, as well as the respective references, to obtain
54 the normalized CSR and the respective adjustment parameters.

55

56

Table 1: Calculation of CSR and adjustment parameters adopted in the present work

Expressions for computation of the parameters	Reference work
$CSR = \frac{\tau_{cyc}}{\sigma'_{v0}} = 0.65 \cdot \frac{a_{max}}{g} \cdot \frac{\sigma_{v0}}{\sigma'_{v0}} \cdot r_d$	Seed and Idriss (1967)
$r_d = e^{[\alpha(z) + \beta(z) \cdot M_w]}$	
$\alpha(z) = -1.012 - 1.126 \sin\left(\frac{z}{11.73} + 5.133\right)$	Idriss (1999)
$\beta(z) = 0.106 + 0.118 \sin\left(\frac{z}{11.28} + 5.142\right)$	
$CSR_{M=7.5, \sigma'_v=1atm} = \frac{CSR_{M, \sigma'_v}}{MSF \cdot K_\sigma}$	Idriss and Boulanger (2008)
$K_\sigma = 1 - C_\sigma \cdot \ln\left(\frac{\sigma'_v}{p_a}\right) \leq 1.1$	Idriss and Boulanger (2008)
$C_\sigma = \frac{1}{18.9 - 2.55\sqrt{(N_1)_{60ks}}} \leq 0.3 \quad \text{or} \quad C_\sigma = \frac{1}{37.3 - 8.27(q_{c1Ncs})^{0.264}} \leq 0.3$	
$MSF = 1 + (MSF_{max} - 1) \left[8.64 \exp\left(\frac{-M}{4}\right) - 1.325 \right]$	Boulanger and Idriss (2014)
$MSF_{max} = 1.09 + \left(\frac{q_{c1Ncs}}{180}\right)^3 \leq 2.2$	

57
58
59
60
61
62
63
64
65
66
67
68
69
70
71
72
73
74
75
76
77
78
79
80
81
82
83
84

On the other hand, the cyclic resistance ratio (CRR) can be estimated from lab and in situ test results. The standard penetration tests (SPT) and cone penetration test (CPT) are particularly convenient, given the extensive worldwide database and past experience. Moreover, the use of the flat dilatometer test (DMT) has been developed in the last two decades, stimulated by the recognised sensitivity of the horizontal stress index K_D to a number of factors which are known to increase liquefaction resistance (difficult to sense by other tests), such as stress history, prestraining/aging, cementation, structure, and by its correlation with relative density and state parameter (Monaco et al. 2005). Shear wave velocities also provide a reliable assessment of liquefaction resistance of soils, since both depend on similar factors, namely confining stresses, soil type, void ratio and relative density (Andrus et al., 2004).

In this work, the proposals of Boulanger and Idriss (2014) based on SPT and CPT have been adopted (Eq. 2 and 3), where $(N_1)_{60cs}$ and q_{c1Ncs} correspond to normalised equivalent clean sand values, as suggested by Idriss and Boulanger (2008). According to these authors, a clean sand is considered to have a fines content (FC) below 5%. It should be noted that the introduction of the FC in these approaches reflects its importance in the liquefaction susceptibility of the soil. However, the estimate of FC based on SPT tests can be ambiguous and may lead to inaccurate results of CRR especially for FC below 25%. Based on Idriss and Boulanger (2008), a correspondence between soil type and FC has been established, as detailed below (section 4.1).

$$CRR_{7.5} = \exp\left(\frac{(N_1)_{60cs}}{14.1} + \left(\frac{(N_1)_{60cs}}{126}\right)^2 - \left(\frac{(N_1)_{60cs}}{23.6}\right)^3 + \left(\frac{(N_1)_{60cs}}{25.4}\right)^4 - 2.8\right) \quad (2)$$

$$CRR_{7.5} = \exp\left(\frac{q_{c1Ncs}}{113} + \left(\frac{q_{c1Ncs}}{1000}\right)^2 - \left(\frac{q_{c1Ncs}}{140}\right)^3 + \left(\frac{q_{c1Ncs}}{137}\right)^4 - 2.8\right) \quad (3)$$

For DMT-based liquefaction analyses, the Marchetti (2016) CRR- K_D curve has been used. Since the effects of higher fines content have not yet been fully investigated and clearly established, all the DMT triggering curves apply to clean sands. Therefore, the CRR is defined by combining the Idriss and Boulanger (2006) CRR- Q_{cn} correlation and the Robertson (2012) average Q_{cn} - K_D interrelationship (Eq. 4), where Q_{cn} is the normalized cone resistance. A combined correlation for estimating CRR based on Q_{cn} and K_D (Eq. 5) was also obtained by Marchetti (2016), by adopting the geometric average between a first CRR estimate obtained from Q_{cn} (Eq. 4) and a second CRR estimate obtained from K_D (introducing K_D into Eq. 4).

$$CRR_{7.5} = \exp\left(\frac{Q_{cn}}{540} + \left(\frac{Q_{cn}}{67}\right)^2 - \left(\frac{Q_{cn}}{80}\right)^3 + \left(\frac{Q_{cn}}{114}\right)^4 - 3\right), \text{ where } Q_{cn} = 25 \cdot K_D \quad (4)$$

$$\text{Average CRR} = [(\text{CRR from } Q_{cn}) \cdot (\text{CRR from } K_D)]^{0.5} \quad (5)$$

85
 86 For the assessment of liquefaction resistance of soils based on shear wave velocities, two methodologies have
 87 been adopted, namely those proposed by Andrus and Stokoe (2000) and Kayen et al. (2013). Andrus and Stokoe
 88 (2000) follow the same approach of the simplified procedure, with CRR computed from the stress-corrected
 89 shear wave velocity in depth (V_{S1}), as follows:

$$90 \quad \text{CRR} = \left[0.022 \cdot \left(\frac{K_{a1} V_{S1}}{100} \right)^2 + 2.8 \cdot \left(\frac{1}{V_{S1}^* - K_{a1} V_{S1}} - \frac{1}{V_{S1}^*} \right) \right] \cdot K_{a2}, \text{ where } V_{S1} = V_S \cdot \left(\frac{P_a}{\sigma'_{v0}} \right)^{0.25} \quad (6)$$

91 where V_{S1} is the normalised shear-wave velocity; K_{a1} and K_{a2} are ageing correction factors on V_{S1} and CRR,
 92 respectively, both corresponding to 1 for uncemented recent soils; V_{S1}^* is the upper boundary value of V_{S1} for
 93 liquefaction occurrence; p_a is the reference atmospheric pressure (=100 kPa) and σ'_{v0} is the initial effective
 94 overburden stress.

95
 96 On the other hand, Kayen et al. (2013) developed probabilistic correlations, based on a vast database of well-
 97 documented case histories, for V_S -based probabilistic and deterministic assessment of liquefaction
 98 susceptibility. In this paper, the deterministic approach has been employed for a liquefaction probability (P_L)
 99 of 15%, using the equations provided below. The respective factors of safety are computed, as before, as the
 100 ratio of the soil capacity to resist liquefaction at P_L (15%) and the corresponding seismic demand, CSR.

$$101 \quad P_L = \Phi \left\{ - \frac{\left[(0.0073 \cdot V_{S1})^{2.8011} - 1.946 \cdot \ln(\text{CSR}) - 2.6168 \cdot \ln(M_w) - 0.0099 \cdot \ln(\sigma'_{v0}) + 0.0028 \cdot (\text{FC}) \right]}{0.4809} \right\} \quad (7)$$




$$102 \quad \text{CRR} = \exp \left\{ \frac{\left[(0.0073 \cdot V_{S1})^{2.8011} - 2.6168 \cdot \ln(M_w) - 0.0099 \cdot \ln(\sigma'_{v0}) + 0.0028 \cdot \text{FC} - 0.4809 \cdot \Phi^{-1}(P_L) \right]}{1.946} \right\}$$

101
 102 Alternative approaches to the assessment of liquefaction potential have been suggested, mainly focusing on
 103 estimates of liquefaction-induced damages, based on quantitative liquefaction risk indexes, namely the
 104 Liquefaction Potential Index (LPI) and the Liquefaction Severity Number (LSN). Originally developed by
 105 Iwasaki et al. (1978), LPI combines the safety factor with depth, z , down to 20 m. Iwasaki et al. (1982)
 106 classification was adopted, as indicated in Table 2, since it is also implemented in CLiq® and the differences
 107 with other classifications are minor. The adopted colour code relative to each LPI class is also included in the
 108 table.

109

110 Table 2: Classification of liquefaction potential based on LPI (after Iwasaki et al., 1982)

LPI	Liquefaction potential
0	<input type="checkbox"/> Very low

$0 < LPI < 5$		Low
$5 < LPI < 15$		High
$15 > LPI$		Very high

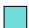

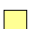

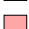

111

112 Tonkin and Taylor (2013) developed another quantitative indicator of the liquefaction-induced damages, the
 113 Liquefaction Severity Number (LSN). This index represents the expected damage effects of shallow
 114 liquefaction on direct foundations, based on post-liquefaction volumetric deformations, associated with
 115 reconsolidation settlements. Using this approach, the liquefaction severity can be classified in terms of expected
 116 damage, according to Tonkin and Taylor (2013), as in Table 3, where the adopted colour scheme is also shown.

117

118

Table 3: Liquefaction severity and damage based on LSN (Tonkin and Taylor, 2013)

LSN range	Typical performance
0 – 10	 Little to no expression of liquefaction
10 – 20	 Minor expression of liquefaction, some sand boils
20 – 30	 Moderate expression of liquefaction, sand boils and some structural damage
30 – 40	 Moderate to severe liquefaction, settlement can cause structural damage
40 – 50	 Major expression of liquefaction, damage ground surface, severe total and differential settlements
> 50	 Severe damage, extensive evidence of liquefaction, severe total and differential settlements affecting structures, damage to services

119

120 2. Selection of the pilot site

121 2.1. Seismicity and liquefaction zonation of Portugal

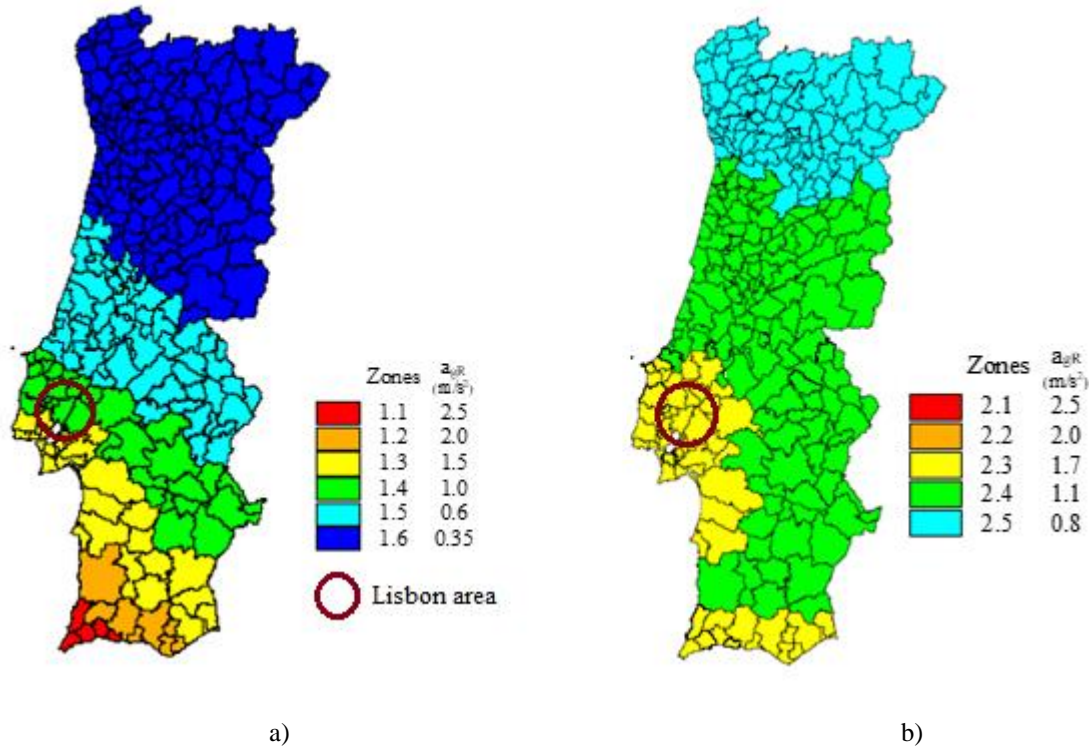
122

123 Portugal’s mainland and its Atlantic coast are located on the western and southern margins of the Iberian
 124 Peninsula. The seismicity of the Portuguese territory is heterogeneous and is classified according to regions
 125 with distinct seismic behaviour. Seismicity increases in intensity from North to South, with a spatial distribution
 126 concentrated in the South and the Atlantic margins. According to existing records, earthquake epicentres are
 127 concentrated near the city of Évora, in the Lisbon region, in the Lower Tagus River Valley region, and along
 128 the Algarve coast (Ferrão et al. 2016). The greater Lisbon area is probably the zone with greater seismic risk,
 129 coincidentally where the capital and largest city of Portugal is located. It is affected by the occurrence of large
 130 moment magnitude ($M_w > 8$) distant earthquakes and of medium magnitude ($M_w > 6$) near earthquakes (Azevedo
 131 et al. 2010). An example of a distant event is the 1755 earthquake ($M_w > 8.5$) generated in the Eurasian-Nubia
 132 plate boundary zone. However, local intraplate ($M_w \approx 6-7$) earthquakes have occurred more frequently, in 1344,
 133 1531 and 1909.

134

135 The Portuguese National Annex of the European Standard for Design of structures for earthquake resistance,
 136 EN 1998-1, Eurocode 8 or EC8-NA (CEN, 2010), established the seismic zonation of continental Portugal, as
 137 shown in Figure 1. This zonation considers two types of seismic actions: Type 1 and Type 2. Type 1 refers to
 138 a “distant earthquake” scenario, corresponding to greater magnitude earthquakes at longer distances (with
 139 epicentre in the Atlantic region), while Type 2 refers to a “near earthquake” scenario, associated with moderate

140 magnitude earthquakes at close distance (with epicentre in the continental territory). According to EC8, seismic
 141 hazard is described in terms of the peak ground acceleration in type A ground (rock), a_{gR} . The values of a_{gR} for
 142 each zone and seismic action type are included in Figure 1. Following these seismic actions, examples of
 143 liquefaction assessment by in situ tests are available in the Algarve (e.g. Rodrigues et al. 2016).
 144

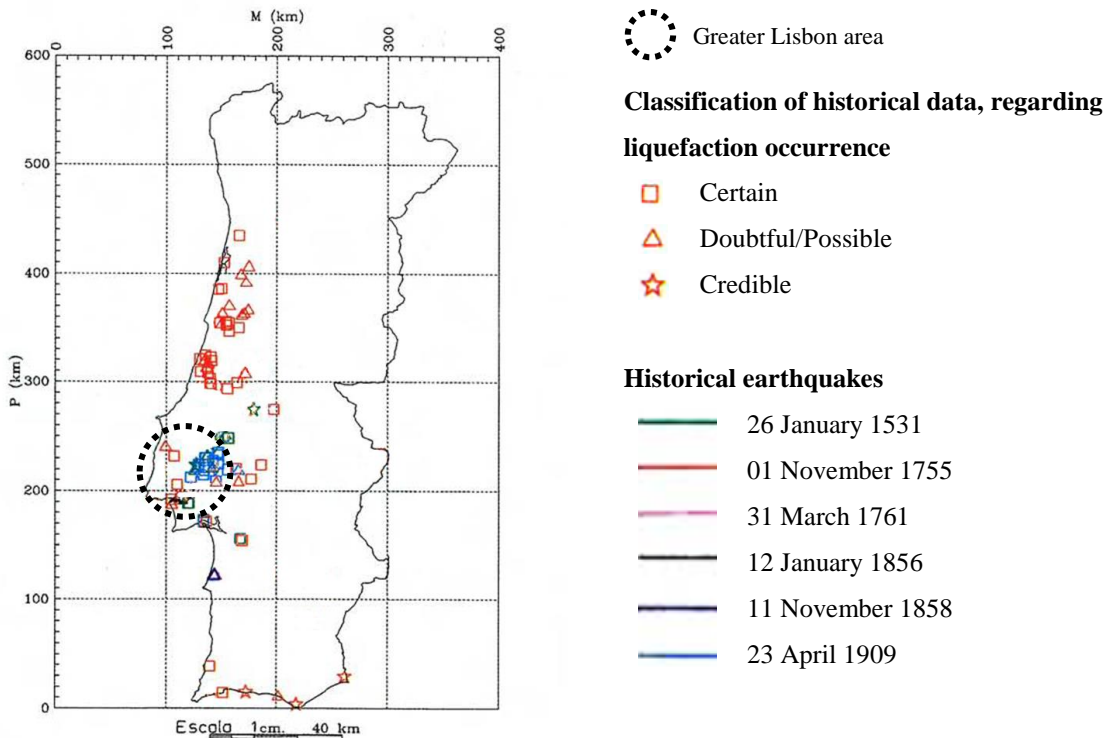


145
 146 a) b)
 147 Figure 1: Seismic zonation of Portugal mainland: a) Action Type 1; b) Action Type 2 (adapted from EC8)
 148

149 Earthquake Induced Liquefaction Disasters (EILDs) are responsible for significant additional structural damage
 150 and casualties, particularly in zones where specific geologic, geomorphological, hydrological and geotechnical
 151 characteristics indicate liquefaction potential of soils below structures (LIQUEFACT, 2017). The presence of
 152 thick profiles of recent alluvial sandy deposits in a high seismicity area is a good example of the combination
 153 of the necessary liquefaction triggering conditions.
 154

155 Information regarding seismic activity in Portugal only started being collected after the 1755 earthquake. For
 156 older events, the available data only include the testimonials of people experiencing large earthquakes. Since
 157 these are mostly subjective descriptions of ordinary people, it has been hard to assess the level of reliability of
 158 this information with reference to liquefaction; this means that doubts arise in several circumstances as to
 159 whether the phenomenon actually occurred. For this reason, as discussed by Jorge (1993), data in the catalogue
 160 are classified in terms of quality of information and localization of the source. In particular, the categories are
 161 ‘certain’, ‘doubtful’, ‘very doubtful’ and ‘credible’ liquefaction. The first three categories refer to descriptions
 162 directly related to liquefaction, with more or less certainty. The ‘credible liquefaction’ category provides
 163 information, not directly describing but potentially related to the liquefaction phenomenon. Following this

164 approach, Jorge and Vieira (1997) identified in the map shown in Figure 2, the locations of historical
 165 liquefaction events coupled with a reliability classification. This is considered the most reliable source of
 166 information on the evidences of the liquefaction phenomenon in Portugal. From the earthquake catalogue, Jorge
 167 and Vieira (1997) identified six earthquake events associated with liquefaction, as indicated in Figure 2:
 168 26/01/1531 (M=7.1); 01/11/1755 (M=8.5); 31/03/1761 (M=7.5); 12/01/1856 (M=6.0); 11/11/1858 (M=7.2)
 169 and 23/04/1909 (M=6.6). The details of these events are listed in Portuguese catalogues, including the
 170 magnitude, macroseismic intensity and coordinates of the epicentre. The locations where liquefaction occurred
 171 as well as the epicentral distances were not reported, but were assumed, according to the site where liquefaction
 172 was observed, even considering the large degree of uncertainty. This uncertainty was reflected in the calculation
 173 of the estimated epicentral distances, however the error made in this computation was taken into account.
 174
 175



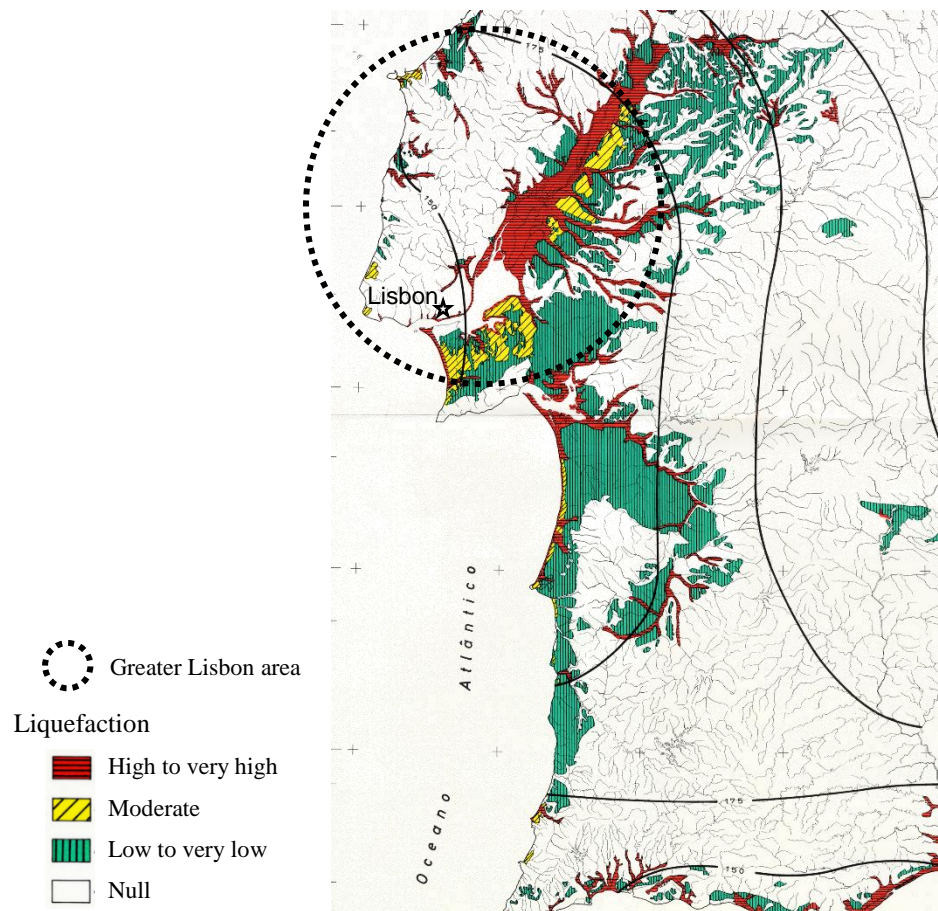
176 Figure 2: Location of liquefaction events associated with historical earthquakes (adapted from Jorge, 1993).

177 Note: “Very doubtful” occurrences have been removed from the original map. PERMISSION GRANTED BY THE
 178 AUTHOR

179
 180 A liquefaction potential zonation map of Continental Portugal was developed by Jorge (1993) and further
 181 discussed by Jorge and Vieira (1997). This zonation map was derived from the superposition and generalization
 182 of two basic maps: the liquefaction ‘opportunity’ map and the liquefaction susceptibility map. For the greater
 183 Lisbon area, a more detailed representation was produced, which evidenced the high liquefaction potential of
 184 that region, as illustrated in Figure 3.

185

186 After the identification of the ‘high to very high’ liquefaction susceptibility areas in Figure 3, mostly along the
187 Lower Tagus Valley, the collection and analysis of existing geotechnical data in that region was carried out,
188 mainly covering the municipalities of Vila Franca de Xira, Benavente, Montijo and Barreiro.
189



190
191 Figure 3: Liquefaction zonation map (Jorge, 1993; Jorge and Vieira, 1997)

192 PERMISSION GRANTED BY THE AUTHOR

193
194 2.2. *Collection and analysis of existing information*

195
196 For the selection of the location of the pilot site, the investigation was initiated with the collection of existing
197 geological and geotechnical information in the metropolitan region of Lisbon along the Lower Tagus River
198 Valley area. With the collaboration of numerous public institutions, governmental agencies, private companies,
199 contractors and design offices, a considerable volume of geotechnical data was assembled. After careful
200 inspection, 95 geotechnical reports were selected for analysis, in a total of more than 350 test results. The
201 majority of these tests, about 72%, corresponded to SPT and borehole logging, in a total of 257 test results, but
202 also included 70 CPT(u), 12 DMT and 17 V_s measurements (from SCPT, Cross-Hole or seismic refraction).
203 Information on the position of the groundwater level at the time of testing was also available in most test reports.
204

205 These reports refer only to the North-East to South part of the Lower Tagus Valley in the Greater Lisbon, where
 206 quaternary sand deposits are expected, involving the municipalities of Vila Franca de Xira, Azambuja,
 207 Salvaterra de Magos, Benavente, Alcochete, Montijo and Barreiro, mostly located along the left bank of the
 208 Tagus river and estuary. Important works associated to the construction of a major highway (A10), including a
 209 12 km extension bridge and viaduct crossing the river Tagus and agricultural plains, have provided a wealth of
 210 information from extensive geological and geotechnical site characterisation tests, which were collected and
 211 analysed for the present research.



212
 213 For the assessment of liquefaction susceptibility in this region, the peak ground acceleration a_{max} was computed
 214 according to EC8-NA (CEN, 2010), as summarised in Table 4.

215 Table 4: Calculation of a_{max} for Vila Franca de Xira and Benavente, according to EC8-NA (CEN, 2010)

Seismic action	Seismic zone	M_w	a_{gR} (m/s ²)	γ_I	a_g (m/s ²)	Ground type	S_{max}	S	a_{max} (m/s ²)	a_{max} (g)
Type 1	'1.4'	7.5	1.0	1	1.0	D	2.0	2.00	2.0	0.20
Type 2	'2.3'	5.2	1.7	1	1.7	D	2.0	1.77	3.0	0.31

216
 217 The analysis of the collected reports was carried out, according to the type of test, based on the previously
 218 described approaches to the assessment of liquefaction susceptibility. The classification of the liquefaction
 219 susceptibility of each soil profile was made, according to two criteria: a) minimum factor of safety of 1.00; b)
 220 minimum thickness of the liquefiable soil layer of 3 meters. Consequently, three classes have been considered:
 221 low, moderate and high. For the purpose of geographical referencing and future microzonation, each test point
 222 was geographically located and colour-coded, according to the adopted colour scheme, introduced in Table 5.
 223 On a first approach, geo-referencing was made by introducing all coordinates on Google Earth®. In order to
 224 aid visual identification of liquefiable areas, the same colour code was associated with paddle icons for SPT
 225 data, diamond paddle icons for CPT data and target circles for CH (cross-hole) data, as schematically shown
 226 in Table 5.

227
 228 Table 5: Susceptibility colour code used for existing data points, based on the factor of safety to liquefaction (FS_{liq})

Susceptibility	Thickness of liquefiable soil layer	Colour code	SPT data	CPT data	CH data
None to Negligible	$FS_{liq} > 1$ ($h_{liq} = 0$ m)	 Green			
Moderate	$FS_{liq} \leq 1$: $0 < h_{liq} < 3$ m	 Orange			
High	$FS_{liq} \leq 1$: $h_{liq} \geq 3$ m	 Red			

229
 230 This colour classification of SPT, CPT and CH data points has been superimposed on the liquefaction zonation
 231 map in Figure 3 (from Jorge, 1993), as illustrated in Figure 4.

232

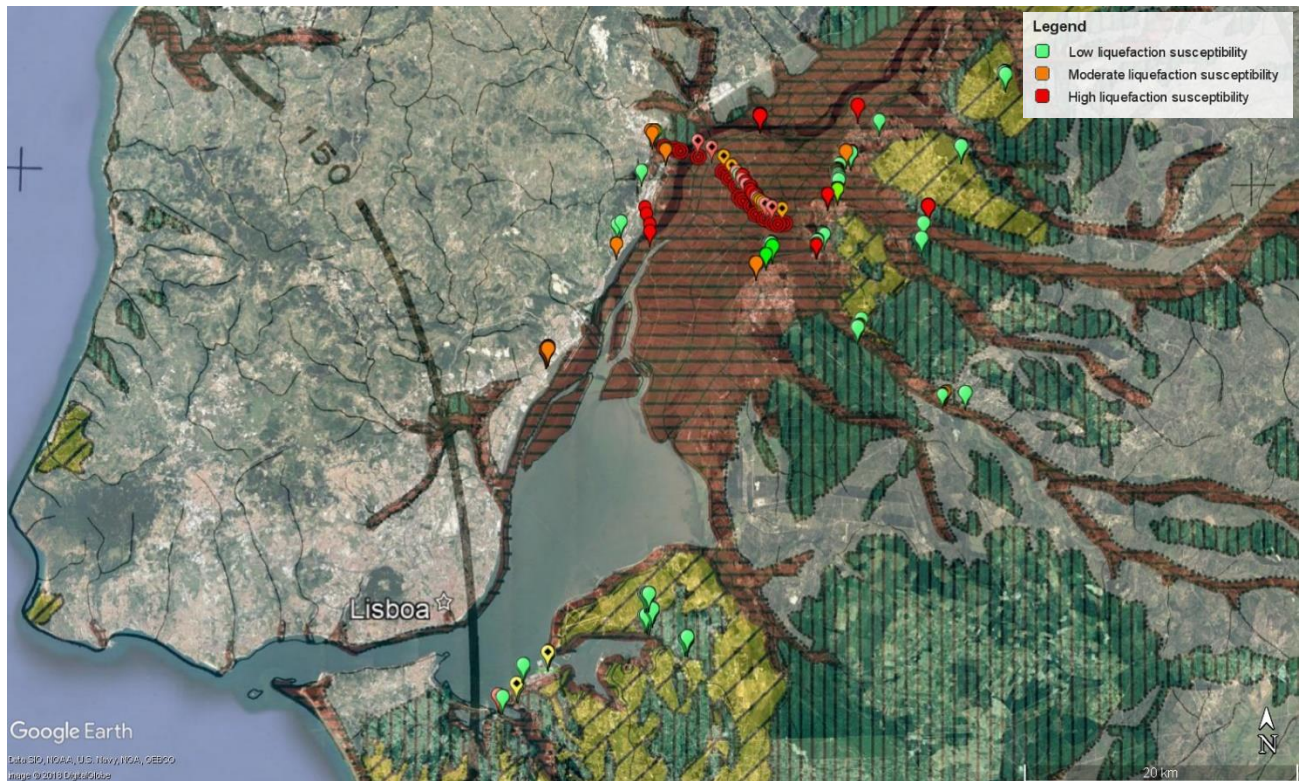


Figure 4: Location of the geotechnical reports collected in the greater Lisbon area, superimposed on the existing liquefaction zonation map (from Jorge, 1993)

233

234

235

236

237 Despite some variability regarding liquefaction susceptibility, there is a substantial agreement between the
 238 general zonation map and the analysed data points. In effect, the red points in Figure 4 are predominantly
 239 located in the area previously identified as having high to very high liquefaction susceptibility, mainly
 240 involving the municipalities of Vila Franca de Xira and Benavente.

241

242 2.3. Location of the pilot site

243

244 The area in the agricultural plains of the “Lezíria Grande de Vila Franca de Xira” was found to have the ideal
 245 geological, hydrogeological and geotechnical, as well as operational conditions, for constituting a research pilot
 246 site on liquefiable soils. The area of the pilot site was divided into zones, named Site Investigation (SI) points,
 247 identified by the respective number. Table 6 summarises the number, type and location of the tests performed
 248 at the pilot site and in each SI, and Figure 5 indicates the testing locations in a map. The location of each type
 249 of tests was selected based on a geological and geomorphological interpretation of the site, described in detail
 250 in Viana da Fonseca et al. (2017) and Saldanha et al. (2018). The position of the groundwater level was
 251 measured in each testing location, which is particularly relevant for liquefaction analyses. An extensive series
 252 of microtremor measurements was also performed, complementary to these investigations, for the purpose of
 253 the liquefaction microzonation of the region, which will not be addressed in this paper.

Table 6: Tests performed in the pilot site

Type of test	Number of tests	Location
Geotechnical	SPT	SI1; SI7
	CPTu	SI1, SI2, SI3, SI4, SI5, SI6, SI7, SI10, SI12, SI13
	SDMT	SI7, SI8, SI9
Geophysical	SASW	SI5
	Cross-Hole (CH)	SI1; SI7 (not considered, see text below)
	Seismic Refraction (SR)	SI1, SI5, SI6, SI7, SI9, SI11, SI12, SI13

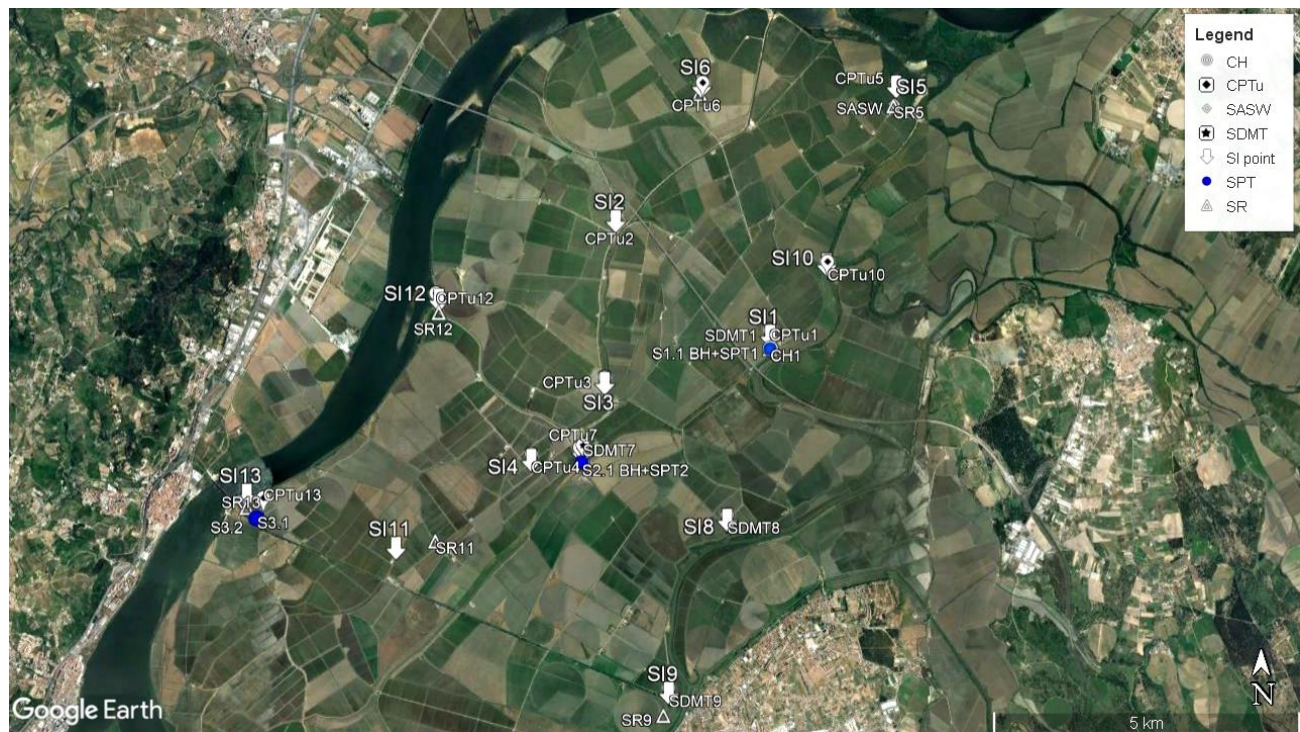


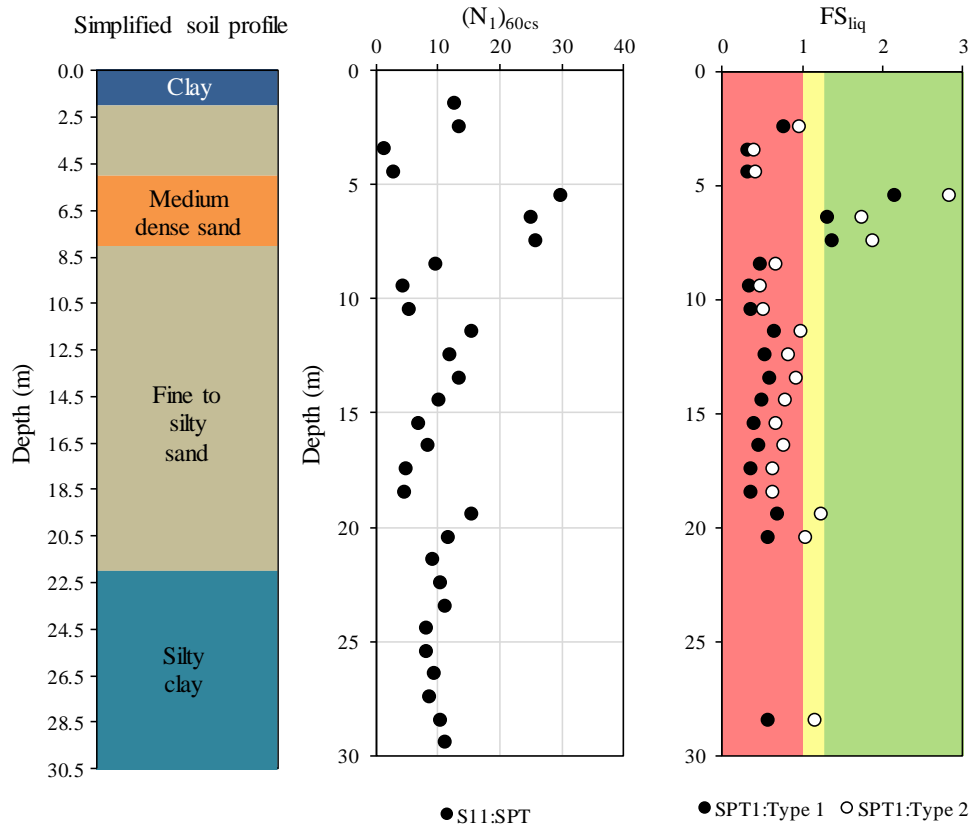
Figure 5: Location of the site investigation (SI) points and of the main tests at the pilot site

259 For the purpose of liquefaction susceptibility assessment from penetration tests, the analysis will focus on SPT,
 260 CPTu and DMT data. For Vs-based liquefaction analysis, direct measurements of SDMT and estimated values
 261 based on SPT, CPT and DMT results will be considered, since CH results were found to be unreliable due to
 262 equipment malfunctioning. On the other hand, surface geophysics results were applied for complementing the
 263 geological and geotechnical characterisation of the site, namely for layer detection, by effectively covering
 264 large areas. The predictions of shear wave velocities from the geotechnical tests were included, given its
 265 valuable contribution to liquefaction analyses, as detailed in Ferreira et al. (2018).

267 3. Characterisation of the pilot site

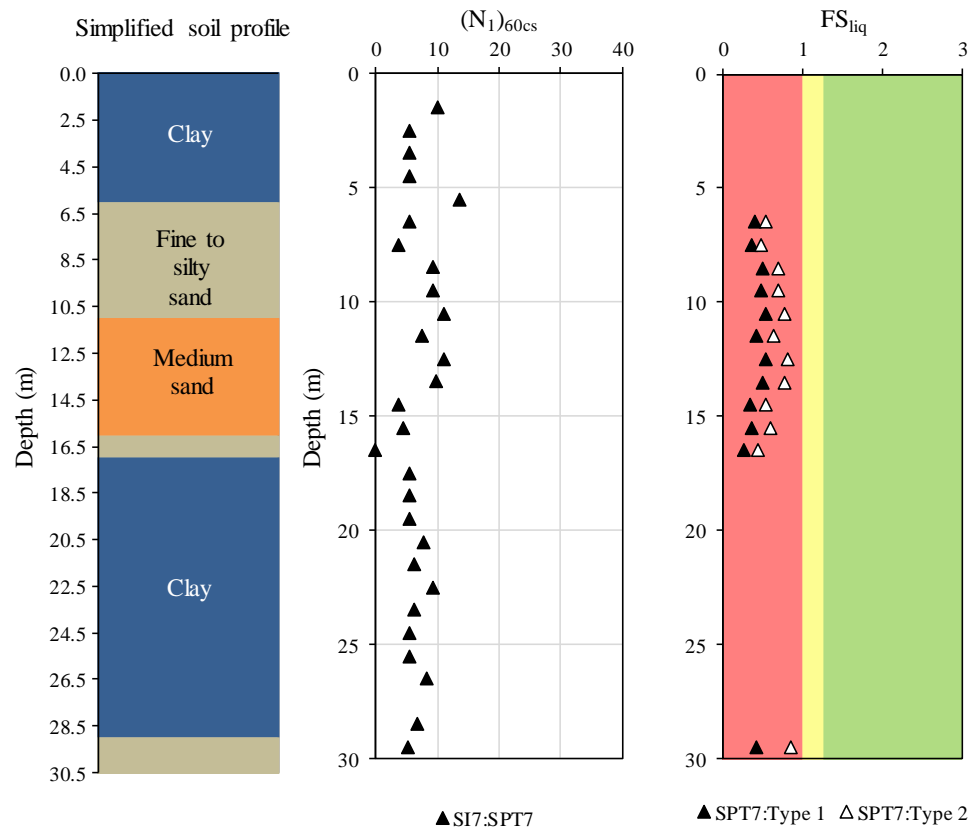
269 3.1. SPT results and preliminary liquefaction assessment

271 Two SPT tests were carried out in SI1 and SI7, respectively. High quality samples were collected in an adjacent
272 borehole, using the Mazier sampler, for complementary laboratory studies. The SPT test results in the two
273 locations in terms of $(N_1)_{60,cs}$ are presented in Figure 6, together with a simplified soil profile defined from the
274 SPT results, as well as a preliminary analysis for liquefaction susceptibility using the simplified procedure,
275 considering Type 1 and 2 seismic actions. The resulting factors of safety against liquefaction refer only to the
276 sandy layers.
277



278

a)



279

b)

280

Figure 6: SPT-based assessment of liquefaction potential at the pilot site: a) SI1; b) SI7

281

282 For clearer perception of the evolution of the factor of safety, FS_{liq} , with depth, 3 coloured zones have been
283 added, corresponding to values below 1.00 (red), between 1.00 and 1.25 (yellow) and above 1.25 (green). The
284 value of 1.00 is conventionally, as previously stated, the minimum factor of safety; however, EC8 is more
285 conservative, proposing a minimum FS_{liq} value of 1.25, hence the transition area in yellow.

286
287 In the illustrated cases of SI1 and SI7 in Figure 6, it is clear that thick sandy layers exhibit high to very high
288 liquefaction susceptibility, except for a medium dense sand layer at 5 to 8 m in SI1. Based on these SPT results,
289 a preliminary liquefaction analysis of each location can be made. At SI1, a non-liquefiable clayey crust of about
290 2m is followed by a 20 m thick liquefiable sandy layer, interbedded by a medium-dense sand layer between
291 5m and 8m, after which a silty clay non-liquefiable layer was found. On the other hand, at SI7, the non-
292 liquefiable clayey crust is 6 m thick and the liquefiable sandy layer is about 11m thick, located between 6 m
293 and 17 m, followed by a clay layer. This analysis will be further discussed by comparison with other
294 geotechnical data.

295

296 3.2. *CPTu testing*

297
298 In this pilot site, ten piezocone tests (CPTu) were performed. The tests were performed according to the ISO
299 22476-1.2012 (ISO, 2012) and the normative procedures proposed by the TC16. The results were treated using
300 the methodology of Boulanger and Idriss (2014) for soil liquefaction analysis, as previously introduced. The
301 groundwater level was measured in each in situ test location, varying from 0.3 m to 2.0 m. The in situ measured
302 values were used in the calculations. Figure 7 shows an example of the CPTu results in three plots: a) cone
303 resistance (q_c) and pore pressure (u_2); b) soil behaviour type index (I_c) and simplified soil profile; c) liquefaction
304 factor of safety (FS_{liq}).

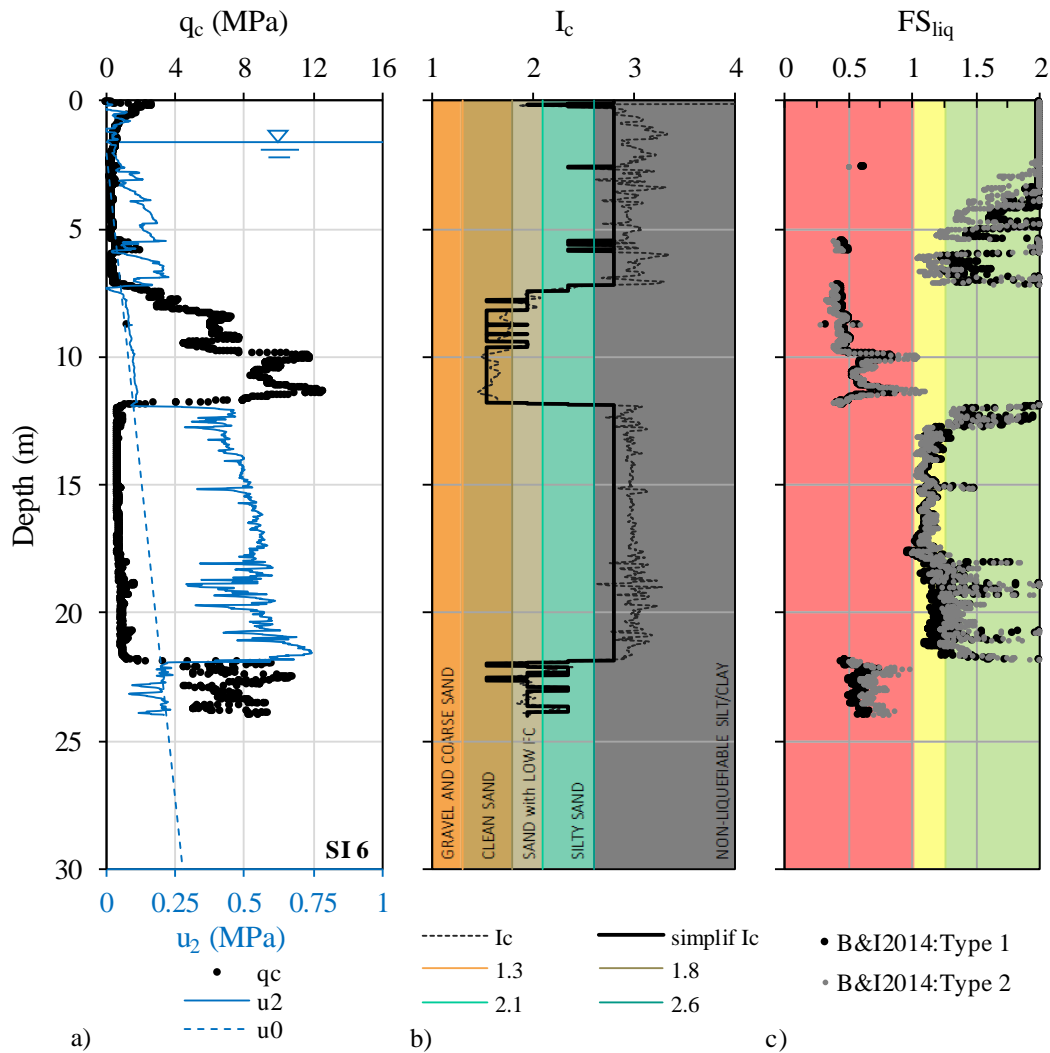


Figure 7: CPTu results in the pilot site at SI6

305

306

307

308 The first plot (Figure 7a) provides the basic information of the soil profile, allowing to distinguish the depths
 309 at which the soil layer is granular (higher cone resistance and pore pressure coincident with the hydrostatic
 310 line) or fine-grained (lower cone resistance and excess pore pressure). The I_c plot (Figure 7b) illustrates a
 311 preliminary soil profile, based on the proposal of Robertson and Wride (1997); in addition, a simplified soil
 312 profile has been defined, by approximating the original I_c by constant values, where similar behaviour is
 313 expected. As proposed by Cubrinovski et al. (2017), the simplified soil profile considers: gravel and coarse
 314 sand ($I_c \leq 1.3$); clean sand ($1.3 \leq I_c \leq 1.8$); sands with low fines content ($1.8 \leq I_c \leq 2.1$); silty sand, sandy silt
 315 and non-plastic silt ($2.1 \leq I_c \leq 2.6$); and, non-liquefiable silt or clay ($I_c \geq 2.6$). This soil classification is different
 316 from the original classification proposal from Robertson (1990), updated by Robertson (2010), as it is focused
 317 on soil response with respect to earthquake-induced liquefaction. From this point of view, there is no distinction
 318 between silts, clays and organic or sensitive soils; instead, these soil types have been grouped together as non-
 319 liquefiable soils. On the other hand, sands have been sub-divided to account for different fines content: from
 320 clean sand to low FC sands, to silty sands, since liquefaction case histories suggest that small variations in fines
 321 content strongly influence liquefaction susceptibility. Finally, Figure 7c illustrates the variation of the factor of

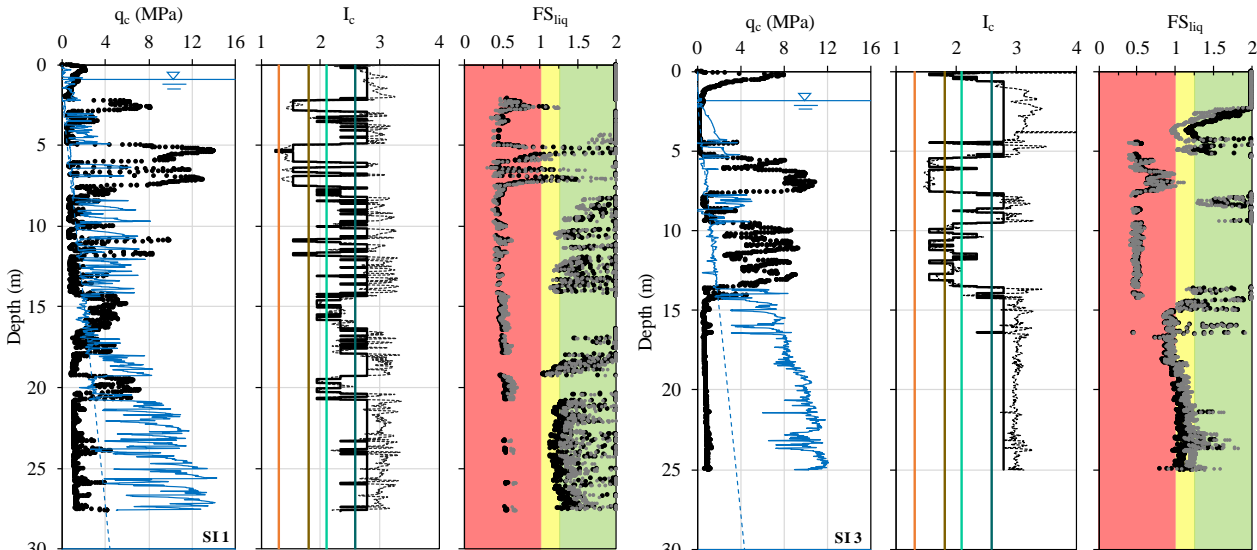
322 safety against liquefaction, FS_{liq} , in depth. Again, coloured zones have been included to ease identification of
323 the critical layers: red for values below 1.00, yellow between 1.00 and 1.25 and green for values above 1.25.

324
325 In the case of SI6, shown in Figure 7, the simplified I_c plot shows distinct soil layers, which can be clearly
326 identified and summarised as follows: a top non-liquefiable layer about 7 m thick, followed by a 5 m thick
327 clean sand layer down to 12 m, then a non-liquefiable layer down to 22 m and a deeper soil layer, consisting of
328 sands with low fines content, again with high liquefaction susceptibility. It should be noted that, below 20 m,
329 liquefaction evaluation is less reliable and should be analysed by means of specific site response analyses, since
330 the uncertainty in some of the computation factors becomes larger (Boulangier and Idriss, 2014).

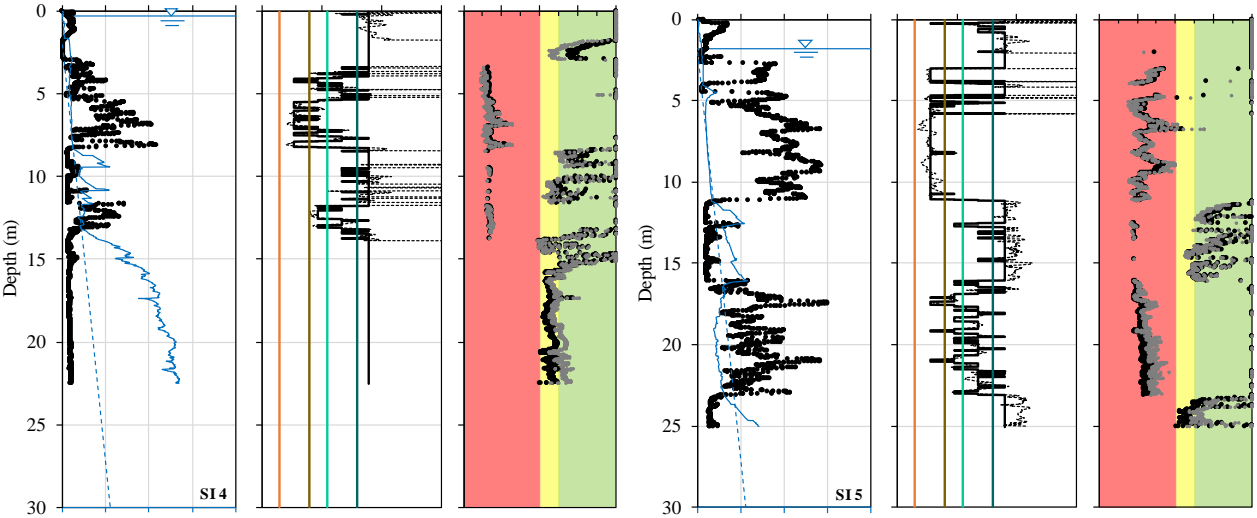
331
332 A general overview of 6 CPTu at different locations within the pilot site are plotted in Figure 8. Thick
333 liquefiable layers can be identified in all of these profiles, despite the significant variability in depth among the
334 different testing locations.

335

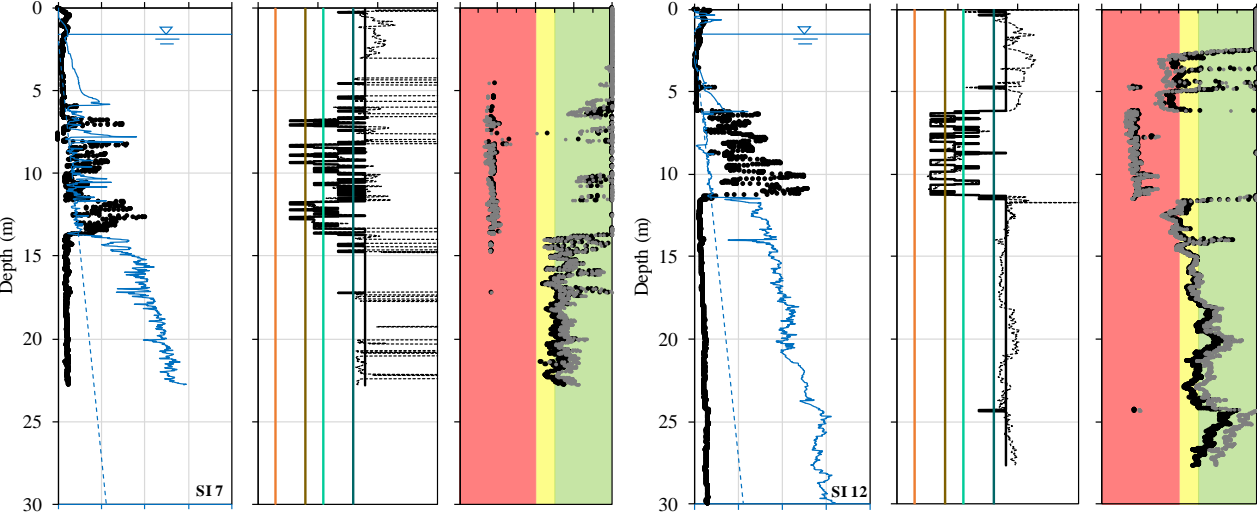
336



337



338



339

Figure 8: Selection of CPTu results in the pilot site at SI1, SI3, SI4, SI5, SI7 and SI12

340



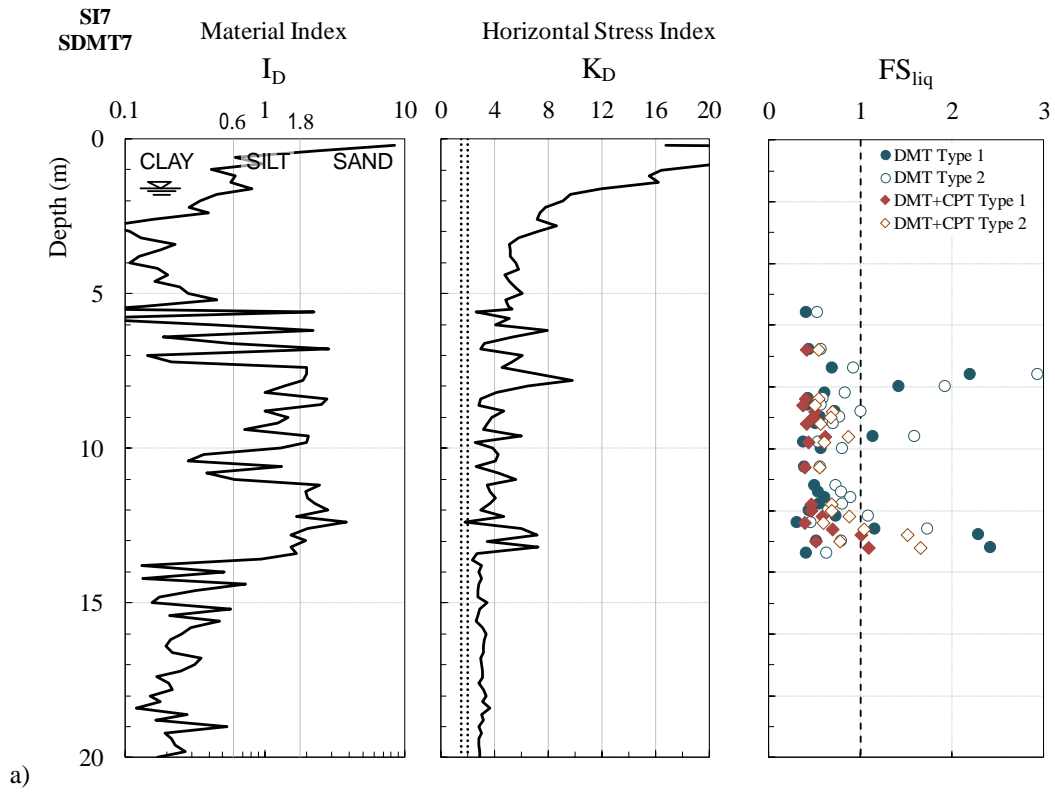
341 3.3. *SDMT testing*

342 In this pilot site, four Seismic Flat Dilatometer tests (SDMT) were performed in the first stage, according to
343 Eurocode 7-Part 3 recommendations and ISO/TS 22476-11. However, at SII, operational problems were
344 experienced, having reached a depth of only 4m. The seismic dilatometer is an extension of the traditional
345 DMT, introduced by Marchetti (1980) with a seismic module implemented above the steel blade (Marchetti et
346 al. 2008). The seismic module consists of an instrumented rod connected between the DMT blade and the rods,
347 equipped with two horizontal geophones spaced 0.50 m, for measuring shear wave velocities, V_s . The presented
348 DMT results were obtained directly from the usual DMT interpretation formulae according to Marchetti (1980)
349 and Marchetti et al. (2001). In this respect, Figure 9 shows the profiles of the material index I_D (indicating soil
350 type) and of the horizontal stress index K_D (related to the stress history) together to the corresponding
351 liquefaction safety factor FS_{liq} at the investigation sites, namely SI7, SI8 and SI9. At each of the sites, FS_{liq} was
352 calculated using the Marchetti (2016) CRR- K_D correlation (DMT data only), while at SI7 DMT and CPT results
353 were combined, according to the Marchetti CRR- K_D - Q_{cn} formulation.

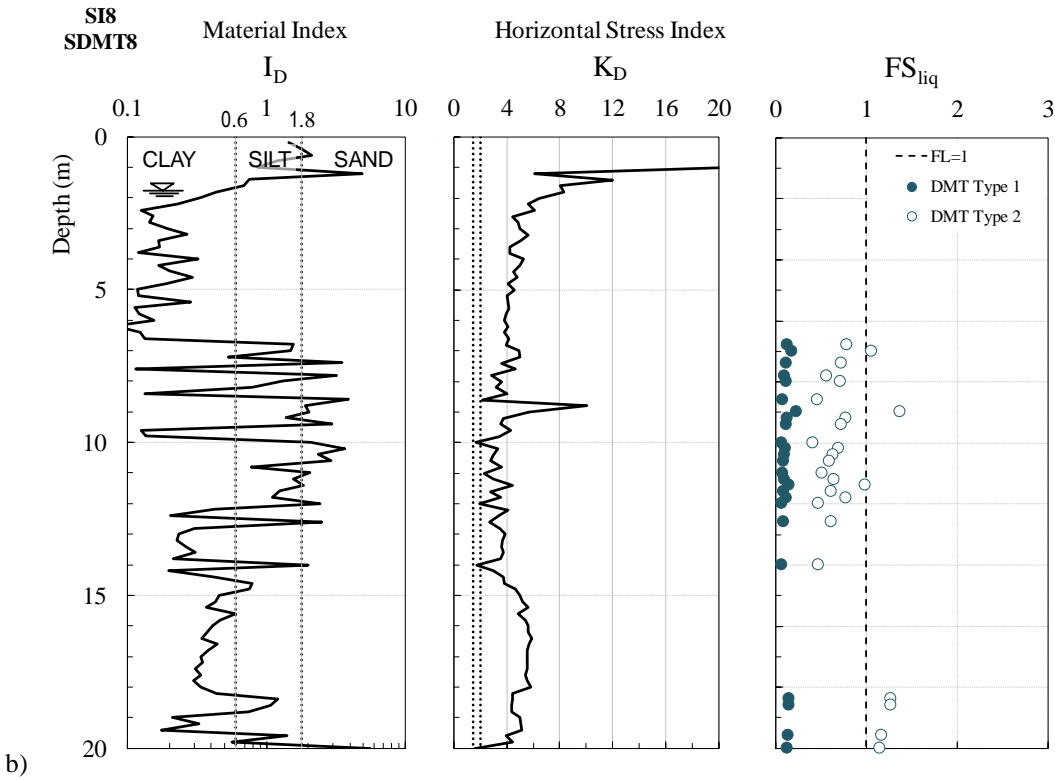
354
355 Comparing with CPT results, DMT liquefaction assessment also detects a non-liquefiable silty-clayey crust of
356 3 to 6 m thickness, depending on the site investigation location, before encountering the sandy and silty-sandy
357 deposits that provide most of the liquefaction down to 14-16 m depth. The combined use of CPT and DMT in
358 SI7 follows the same DMT tendency, even though the liquefaction susceptibility appears to be much lower,
359 probably due to the presence of interbedded layers that do not allow a correct coupling of DMT and CPT data
360 at certain depths.

361

362



363



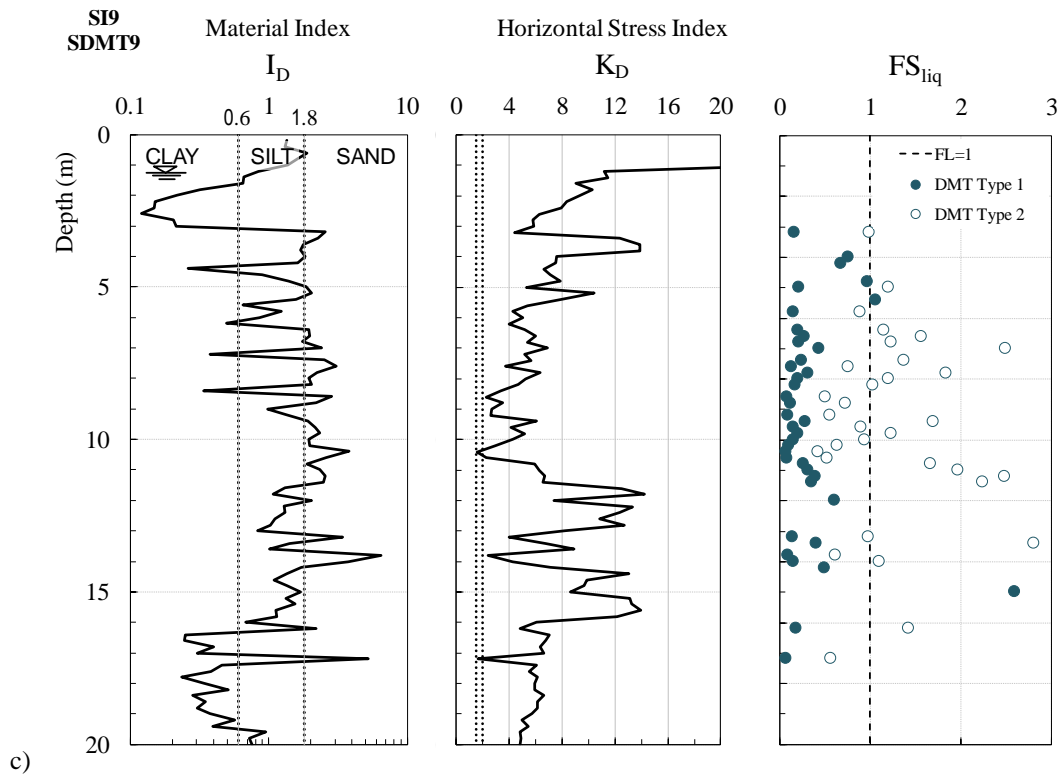


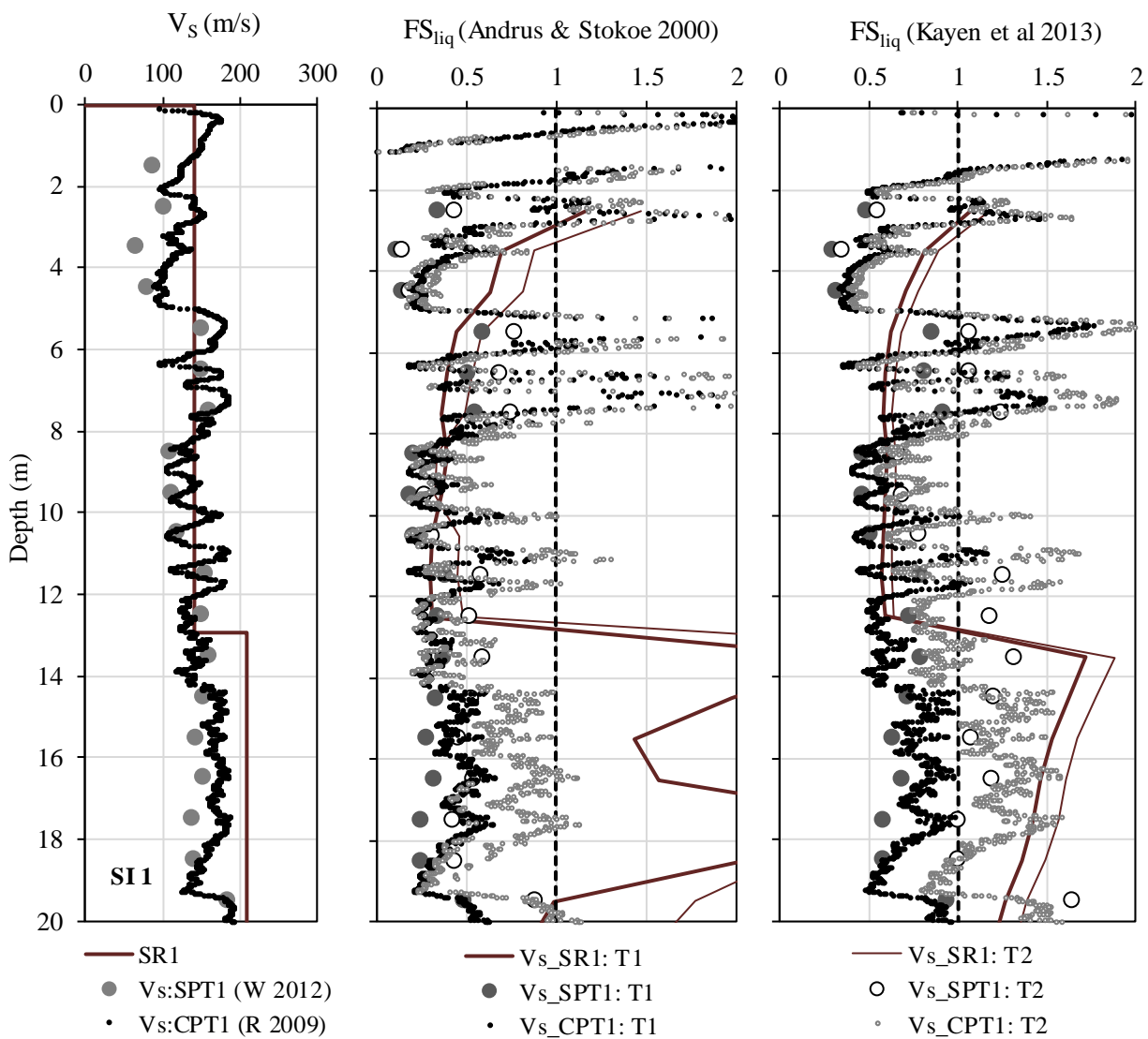
Figure 9: SDMT results in the pilot site: a) SI7; b) SI8; c) SI9

3.4. Geophysical investigations

Seismic wave velocities were measured in the pilot site by means of geophysical surface wave methods, namely via seismic refraction (SR), spectral analysis of surface waves (SASW), as well as in borehole tests, such as the seismic dilatometer (SDMT) and cross-hole (CH) tests. For the purpose of liquefaction assessment, the results of seismic refraction tests were also considered, despite being better suited for profiling and layer detection, by identifying changes in seismic wave velocities in depth. However, borehole seismic tests are considered more reliable and detailed and were analysed, based on direct measurements of V_s , as well as its prediction from penetration tests. In effect, from the variety of in situ penetration tests performed at the pilot site, it was possible to obtain predictions of V_s from correlations with SPT, CPTu and DMT test results. For the SPT- V_s correlations, the proposals of Wair et al. (2012) for different soil types were used, which also take into account the effective vertical stress at each depth of the soil profile. For CPT- V_s correlations, the proposals of Hegazy and Mayne (1995), Mayne (2006), Andrus et al. (2007), Robertson (2009) and McGann et al. (2015) were analysed. As detailed in Ferreira et al. (2018), the prediction proposed by Robertson (2009) was found to be the most appropriate for these soils. For V_s predictions based on DMT, the proposal of Marchetti et al. (2008) was adopted. Amoroso (2014) demonstrated that the DMT-based predictions are more consistent than those based on the CPT. For this analysis, Figure 10 presents the results obtained at SI1 and SI7, in terms of measured V_s via SR and SDMT, as well as estimated V_s profiles based on:

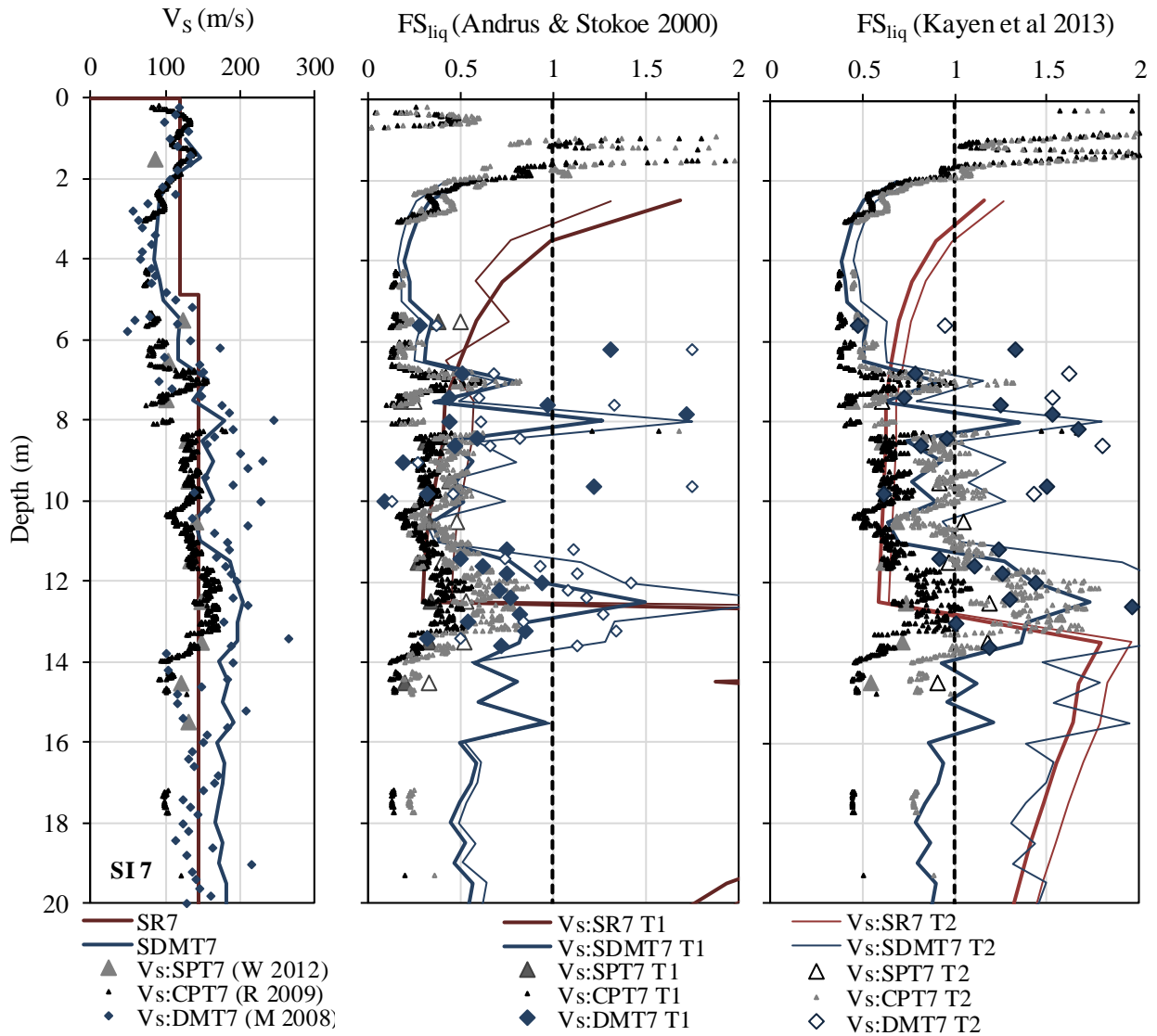
- 386 • Wair et al (2012): SPT (W 2012)
- 387 • Robertson (2009): CPT (R 2009)
- 388 • Marchetti et al. (2008): DMT (M 2008)

389
 390 Figure 10 also includes the computed factors of safety against liquefaction using the two distinct approaches:
 391 Andrus and Stokoe (2000) and Kayen et al. (2013) for the two seismic actions (T1 and T2), taking into account
 392 the estimated fines content.



393 a)

394



395 b)

396

397

Figure 10: Measured and estimated V_s results and respective FS_{liq} : a) SI1; b) SI7

398

399

400

401

402

403

404

405

406

407

408

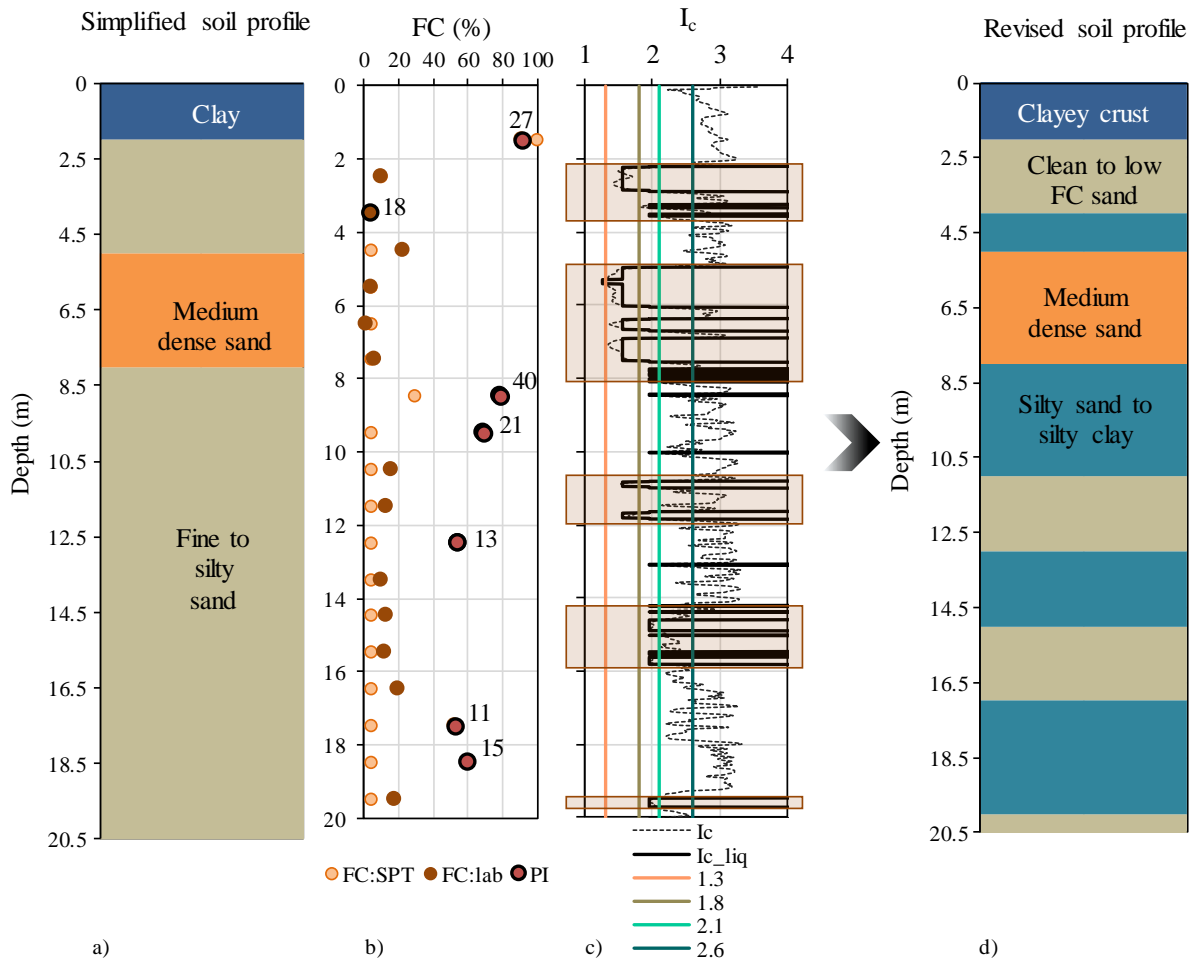
409

In both locations, the results show significant approximation between measured and predicted V_s values. As expected, seismic refraction provides simplified profiles, assuming a stiffness increase with depth, which is not always the case in SI7, as shown in the SDMT profile. DMT-based predictions are remarkably similar with SDMT measurements, which demonstrates the good performance of Marchetti et al. (2008) proposal. As evidenced by Amoroso (2014), DMT-based predictions appear to be more consistent than those based on the CPT considering that DMT- V_s correlations include the horizontal stress index K_D , noticeably reactive to stress history, prestraining/aging and structure, scarcely detected by cone tip resistance q_c from CPT. On the other hand, CPT- V_s predictions are subjected to the additional uncertainty arising from the selection of which one of the numerous existing correlations is adopted, depending on geological age, cementation, effective stress state. With regard to the liquefaction susceptibility assessment, the obtained FS_{liq} values are indicative of very thick liquefiable soils at both locations. However, in SI7, there are significant discrepancies in the results, which are likely linked to the soil type consideration and estimate of fines content, based on FC , I_c and I_D , respectively.

410 **4. Analysis and discussion**

411 *4.1. Combining field and laboratory data*

412 For comparing the results of these field tests, especially in terms of liquefaction susceptibility assessment, two
413 site investigation locations were selected: SI1 and SI7. In order to specifically address the impact of soil type,
414 especially fines content, the laboratory results of grain size distribution and plasticity, obtained on SPT samples,
415 have been integrated in the SPT-based liquefaction assessment. Figure 11a shows the first 20 m of the
416 simplified soil profile in SI1, and Figure 11b presents the comparison between the SPT-estimated and
417 laboratory measured fines content and plasticity index. The SPT-estimated FC were defined, considering the
418 proposal by Idriss and Boulanger (2008), and based on the lithological description of the SPT log (below 5%
419 for clean sand; 5%-10% for sand with fines; 10%-30% for silty sand; above 30% for fine non-liquefiable soils).
420 In addition, the soil type parameter I_c from CPT_u , with a cut-off at 2.35 (average value between 2.1 and 2.6)
421 corresponding to the midpoint between silty sands and non-liquefiable soils, is provided in Figure 11c. The
422 combination of field and laboratory data enabled to redefine the soil profile, by identifying the sandy layers,
423 potentially susceptible to liquefaction, as illustrated in Figure 11d.



424
425

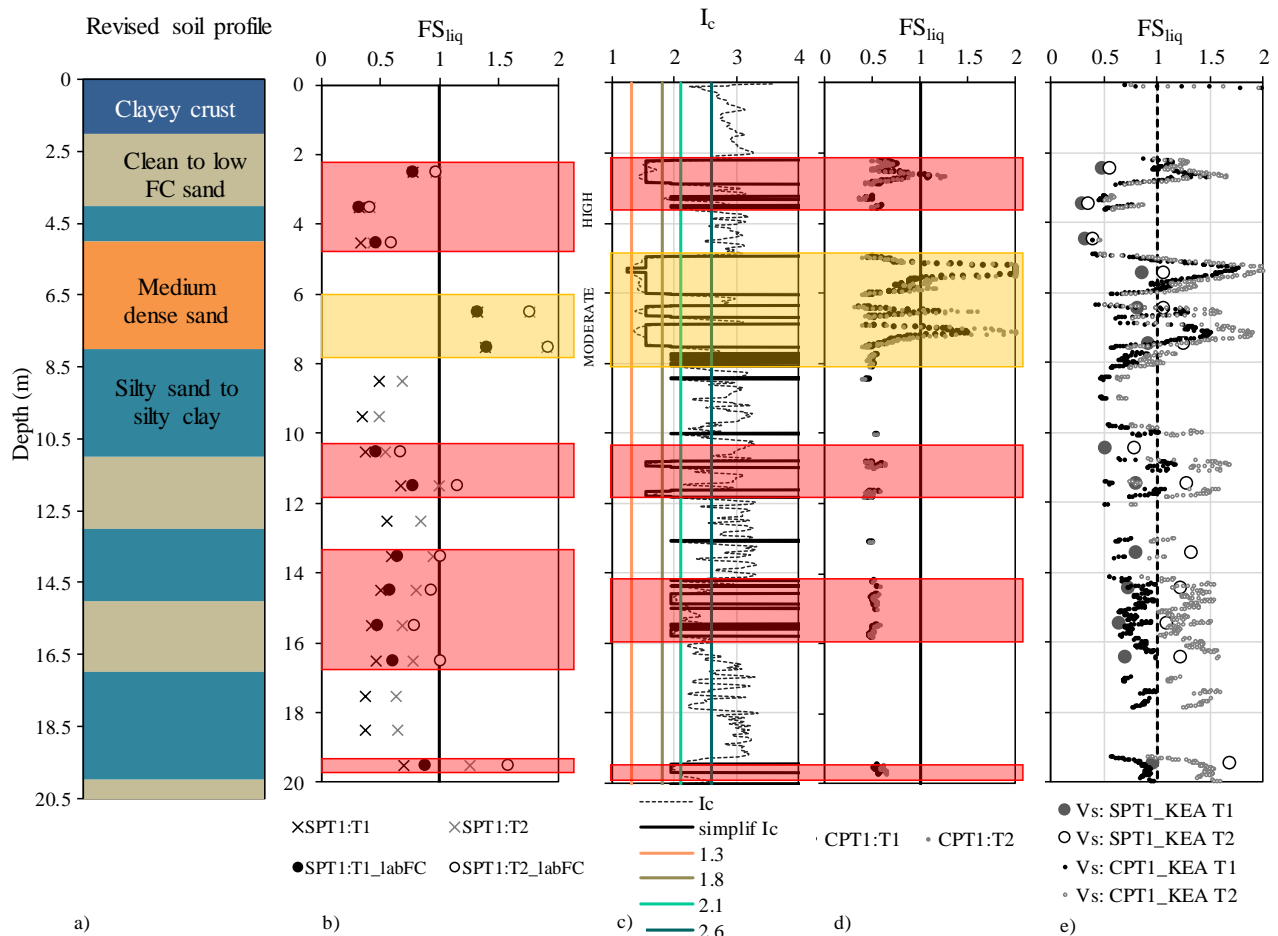
Note: where PI is not specified means non-plastic (NP) soil

426 Figure 11: S11 results: a) SPT simplified soil profile based on lithology; b) SPT-estimated and lab-measured fines
427 content; b) simplified I_c for liquefaction; d) revised soil profile

428
429 The most striking observation, at first glance, is that the revised soil profile is more complex and stratified than
430 the simplified profile derived from the lithological description of the SPT. This is due to the laboratory
431 measurement of fines content, which provides a very different outline of the soil type, as shown in Figure 11b.
432 In this figure, the plasticity indexes at different depths are also included, which are relevant in liquefaction
433 analyses (Boulanger and Idriss, 2014). It is clear that the SPT test alone fails to identify the existence of clay/silt
434 layers interbedded with the sand deposits, which have a very significant impact in the liquefaction response of
435 the profile, so the use of complementary information, especially from the laboratory analysis of the collected
436 SPT samples, is highly beneficial.

437
438 Based on this revised soil profile and using the laboratory-measured fines content information, the factors of
439 safety against liquefaction obtained from SPT, as well as from the estimated V_{S-SPT} and V_{S-CPT} profiles
440 (Kayen et al. 2013 approach) have been recalculated, as indicated in Figure 12, from which the critical layers
441 can be easily identified. In addition, the CPT_u profile has also been revised, by removing FS_{liq} values for I_c

442 above 2.35 (midpoint between silty sands and non-liquefiable soils). For clarity, the results from seismic
 443 refraction tests were not included in this comparison.



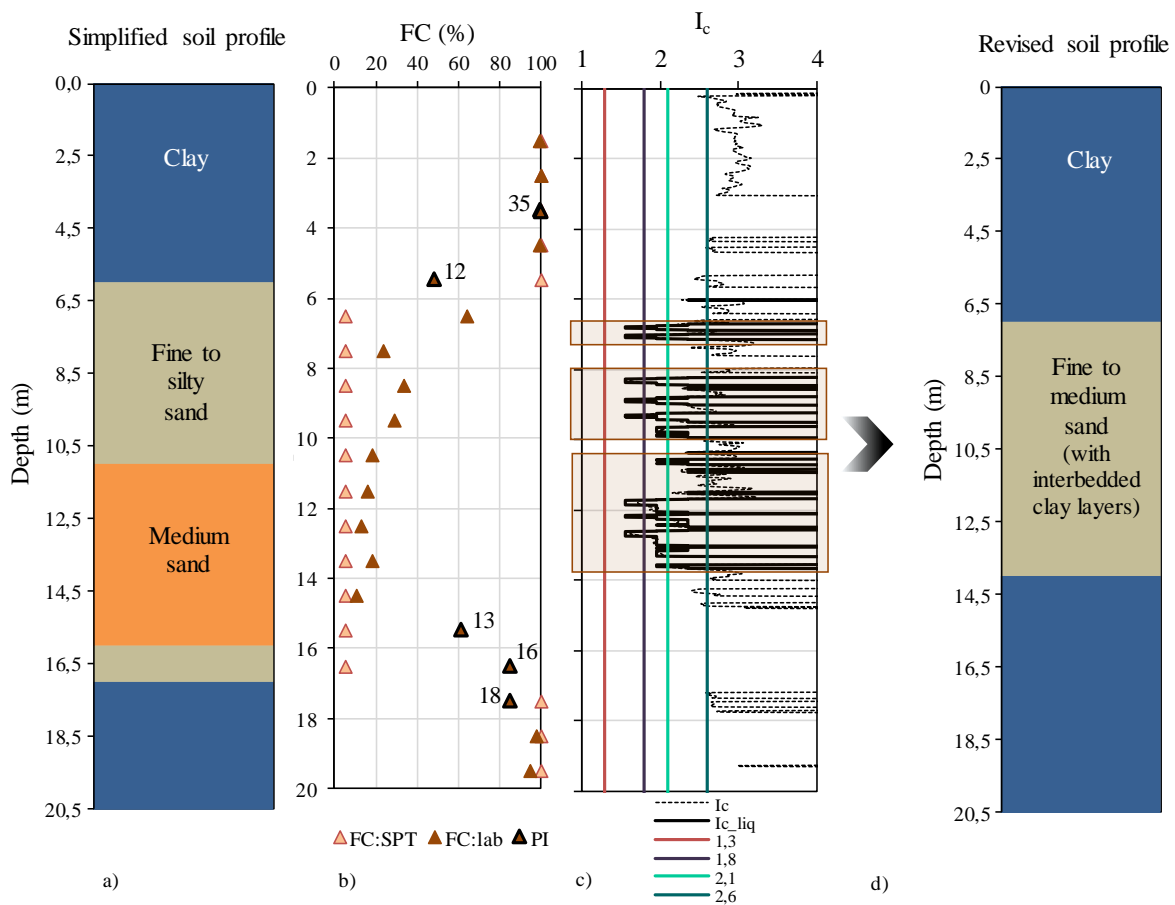
444
 445 Figure 12: Identification of critical layers in SI1 taking FC into account: a) revised soil profile; b) SPT FS_{liq} ; c) revised
 446 I_c ; d) CPTu FS_{liq} ; e) V_s FS_{liq}

447
 448 In contrast with the FS_{liq} profiles in Figure 6a and Figure 8 (SI1), the consideration of the adjustments in fines
 449 content enabled a clearer distinction between layers, particularly useful in the identification of the critical ones.
 450 In this case, a layer of moderate to low liquefaction susceptibility was also detected. Despite the larger scatter
 451 in the V_s -based FS_{liq} profiles, the same critical layers can be recognised, mainly for T1 seismic action. For the
 452 lower magnitude seismic demand (T2), the V_s - FS_{liq} profiles are substantially higher, suggesting that the
 453 computed DWF (Distance Weighting Factor, similar to MSF) may need further adjustments.

454
 455 In sum, in this location, three highly liquefiable layers have been identified, between 2 and 5 m, then at 10 to
 456 12 m, and then from 13 to 17 m. A very thin deep liquefiable layer was also found nearly at 20 m, which effect
 457 at the surface is expected to be negligible. Since the SPT and CPT tests were performed very close to each
 458 other, the discrepancies in the results can only be attributed to the nature and specificities of the in situ test, as
 459 it is necessarily the same soil profile. Since the CPT measurements are nearly continuous (every 1 cm), while
 460 the SPT was performed at every 1 m in depth, the observed differences are a reflection of the many

461 intercalations of fine layers, which often are not visible in the SPT results. In fact, the CPT results show some
 462 points where the FS is high, as well as the SPT results. What is apparent from this comparative analysis is that
 463 the greater detail of the CPT is fundamental to identify these heterogeneous soil profiles, while the SPT may
 464 lead to a different perception of the soil profile.

465
 466 For the second site at SI7, a similar analysis was performed, as outlined in Figure 13, with simplified SPT soil
 467 profile of the first 20 m (Figure 13a), the SPT-estimated (from the lithological description of the SPT log) and
 468 lab-measured fines content (Figure 13b), CPTu soil type profile from I_c ((Figure 13c). Combining this
 469 information, a revised soil profile has been produced (Figure 13d).



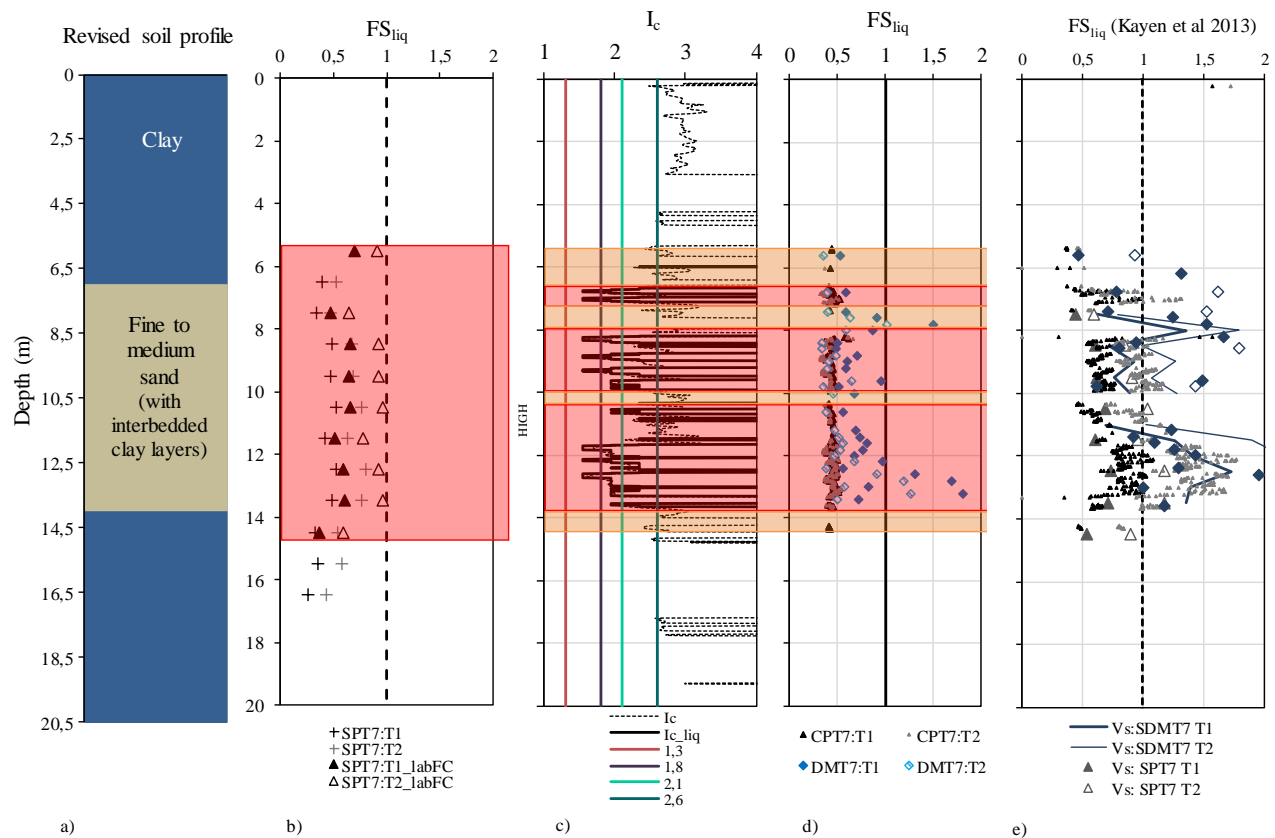
470

471 Note: where PI is not specified means non-plastic (NP) soil (for $FC < 50\%$)

472 Figure 13: SI7 results: a) SPT simplified soil profile based on lithology; b) SPT-estimated and lab-measured fines
 473 content; c) simplified I_c for liquefaction; d) revised soil profile

474
 475 In this case, the original soil profile has been converted into a simpler three-layered profile, despite the existence
 476 of thin interbedded layers of finer soil, as noted in the soil type description. The comparison between SPT-
 477 estimated and laboratory-measured fines content reveals clear differences, as before, particularly near the
 478 interface of the layers. The integration of this information in the revised computation of the factors of safety is

479 illustrated in Figure 14, which also includes the identification of the critical layers in terms of liquefaction
 480 susceptibility.



481 a) b) c) d) e)

482 Figure 14: Identification of critical layers in SI7 taking FC into account: a) revised soil profile; b) SPT FS_{liq} ; c) revised
 483 I_c ; d) CPTu and DMT FS_{liq} ; e) V_s FS_{liq}

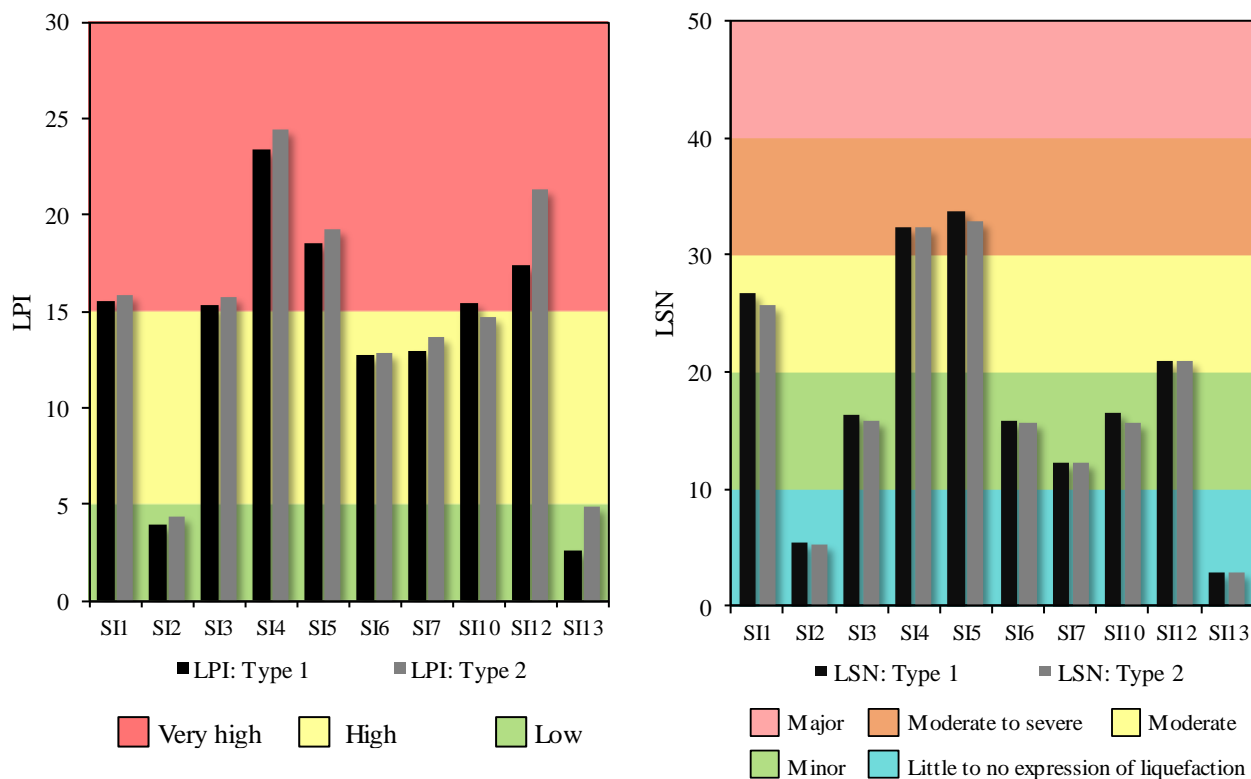
484

485 In this location, the simplified soil profiles from SPT and CPT are relatively similar, with two clayey layers at
 486 the crust and below about 16 m, and a central critical zone. However, the estimate of the thickness of the sandy
 487 layers slightly differs: the SPT results identified about 10 m of liquefiable sands (between 5 and 15 m), while
 488 the CPT indicates about 7 m of sandy soils (from 7 to 14 m), with a few interbedded layers of fine soil. In turn,
 489 DMT results suggest that the liquefiable layer is about 9 m thick, located from 5 to 14 m in depth. As highlighted
 490 in the figure, the combination of these results suggests that it is reasonable to consider a thick liquefiable layer,
 491 approximately between 6 and 15 m. With regard to V_s -based FS_{liq} results, a good agreement with the previous
 492 plot is evident, especially after the FC adjustment obtained from the laboratory measurements (by comparison
 493 with the V_s - FS_{liq} profile in Figure 10b). It is again discernible that the inclusion of soil type information, such
 494 as from laboratory analyses, is vital to obtain a reliable V_s -based assessment of liquefaction susceptibility,
 495 clearly improving its capability for identifying liquefiable and non-liquefiable soil layers.

497 4.2. Overview of the liquefaction response of the pilot site

498 As discussed in the introduction, the use of alternative and quantitative liquefaction indexes is advocated,
 499 providing relevant information in terms of the damage induced by soil liquefaction. For this purpose, LPI and

500 LSN values have been computed, from the field penetration test data, namely SPT, CPT and DMT. At first, it
 501 is worth comparing all the results obtained at the pilot site from CPT data, as presented in Figure 15. In this
 502 figure, LPI and LSN have been calculated considering the two types of seismic actions and a coloured
 503 background shading has been included, based on the classification of Tables 1 and 2.



504
 505 Figure 15: Severity damage based on LPI and LSN from CPTu at the pilot sites
 506

507 As shown in Figure 15, LPI values fall on the high or very high liquefaction severity, except for SI2 and SI13,
 508 where the LPI is low. SI4 appears to be the location with the highest liquefaction susceptibility, in terms of
 509 LPI, but SI5 and SI12 are also classified as highly liquefiable. In sum, from LPI results, it can be concluded
 510 that the majority of testing points exhibit high (50%) to very high (30%) liquefaction severity. In turn, based
 511 on the LSN results in Figure 15, greater surficial liquefaction-induced damages are expected in SI4 and SI5,
 512 however the values fall within the moderate to severe class, that is, below 40. In terms of the variability of LSN
 513 values, there is greater scatter in its classification, with about 20% of the testing points in each class. Since LPI
 514 and LSN are liquefaction severity indicators, some authors have proposed a parallelism between them, namely
 515 Wotherspoon et al. (2015), who made use of the observed superficial manifestations after the Christchurch
 516 series of earthquakes to establish the comparison. The proposed classification relationship is provided in Table
 517 7.

Table 7: Classification of liquefaction severity and damage based on LPI and LSN

Risk Index	Superficial manifestation severity		
	None to Minor	Moderate	Major to Severe
LPI	LPI<5	5<LPI<15	LPI>15
LSN (Wotherspoon et al., 2015)	LSN<20	20<LSN<50	LSN>50
LSN (based on these results)	LSN<10	10<LSN<20	LSN>20

519

520 However, the results in Figure 15 do not fit well within the relationship between LPI and LSN proposed in
521 Table 7, mainly because the LSN values are relatively low, classifying liquefaction severity at all testing
522 locations as minor to moderate, in relation to the relative LPI, which indicates most testing locations as severely
523 affected by liquefaction. Based on the available information, it is not yet possible to state which severity index
524 is being poorly estimated at the pilot site, though it appears that LPI is over-conservative and LSN is possibly
525 unconservative. This poor correspondence, also observed by Wotherspoon et al. (2015) and Cubrinovski et al.
526 (2017), suggests that further studies are required, not only in terms of the liquefaction assessment procedures
527 from which these indices are computed, but also to account for the configuration of the soil profile, namely the
528 thickness of the crust, the depth and thickness of the liquefiable layers, as well as the relative distribution of
529 liquefiable layers and interbedding with fine non-liquefiable layers (Millen et al., 2019). An adjustment based
530 on these test results to the LPI versus LSN classification is also included in Table 7.

531

532 It is also interesting to compare these CPT-derived indexes with those from SPT, DMT, DMT combined with
533 CPT tests, as well as from direct V_s measurements, summarised in Table 8 for LPI and LSN. The results show
534 considerable differences between the absolute values of LPI and LSN, according to the type of test from which
535 these have been computed.

536

537 Table 8: Comparison of LPI and LSN values from SPT, CPTU and SDMT at SI1 and SI7

Seismic action	Type of test	LPI		LSN	
		SI1	SI7	SI1	SI7
Type 1	SPT	31.71	26.52	85.65	51.84
	SPT_lab FC	27.21	23.33	73.59	45.51
	CPT	15.58	12.95	26.74	12.17
	DMT	--	9.65	--	12.30
	DMT+CPT	--	7.70	--	10.25
	V_s_{AS} *	--	43.12	--	--
	V_s_{KAE}	--	26.19	--	--
Type 2	SPT	20.58	17.19	83.97	51.84
	SPT_lab FC	18.24	12.69	68.24	39.88
	CPT	15.88	13.72	25.79	12.17
	DMT	--	5.47	--	10.90
	DMT+CPT	--	4.88	--	9.54
	V_s_{AS}	--	42.78	--	--
	V_s_{KAE}	--	18.09	--	--

* V_s_{AS} (Andrus and Stokoe 2000); V_s_{KAE} (Kayen et al. 2013)

538

539

540 These results suggest that the use of SPT data and V_s measurements for LPI or LSN estimates may lead to
541 significant deviation from realistic values, especially in the presence of interbedded layers of sands and silty
542 clays, as in the present case. Both the original and revised values of $SPT-FS_{liq}$ have been included (SPT and
543 $SPT_{lab FC}$, respectively) to demonstrate the positive impact of the use of laboratory analyses of SPT samples
544 in the improvement of SPT-derived parameters. From a qualitative perspective, the values from SPT and CPTu
545 indicate similar trends, with higher values at SI1. On the other hand, the values of LPI and LSN obtained from
546 DMT and CPT predictions appear reasonably similar, while the combined use of DMT and CPT provides lower
547 indexes, probably due to the abovementioned interbedded layers that does not allow the correct coupling of
548 DMT and CPT data at each soil depth. Given the inadequacy of V_s to distinguish between sandy and clayey
549 soils, the use of V_s -based liquefaction indexes should only be used when specific soil type information (grain
550 size distribution and index properties from laboratory analyses or I_c from CPTu) are available, otherwise these
551 can be largely overestimated. The combination of V_s results with other geotechnical data on soil type proved
552 to be a reasonable alternative solution to overcome this limitation. However, the corresponding LPI values are
553 still overestimated in comparison with those from CPTu.

554

555 **5. Conclusions**

556 A new pilot site in liquefiable soils has been setup in the Greater Lisbon area, which has provided a wealth of
557 geological, geophysical and geotechnical data to be explored and analysed, mainly in terms of liquefaction
558 assessment protocols. The selection of its location is discussed in detail, based on the collection and analysis
559 of existing geological and geotechnical reports. The conventional approach to liquefaction susceptibility
560 assessment, based on the simplified procedure applied to SPT, CPT, DMT and V_s measurements, has been
561 implemented, in terms of the factors of safety against liquefaction (FS_{liq}). The investigated area is constituted
562 by very heterogeneous soil profiles, with interbedded sand-silt-clay layers. In some locations, more
563 homogeneous layers of sand were found and some critical layers were identified, at different depths. However,
564 the profiles are generally very heterogeneous, which is why the use of different in situ tests is even more
565 relevant. In both SI1 and SI7, thick potentially liquefiable layers were found, as well as in many others (see
566 Figure 8) so it can be concluded that the pilot site area is prone to liquefaction.

567 Due to the presence of interbedded layers of sand and clayey soils, some discrepancies were observed in the
568 results, particularly from direct interpretation of SPT and V_s results. This is a consequence of the lack of
569 specific information on soil type, namely fines content, from these test results, which has a strong impact in the
570 assessment of liquefaction susceptibility. To overcome these limitations, laboratory data from physical
571 identification and grain size distribution obtained on SPT samples, were combined with field data, which
572 considerably improved the convergence and the consistency of different test results. In effect, after the inclusion
573 of laboratory measured fines content, it was possible to clearly identify the critical, highly liquefiable layers
574 from the different tests. The analysis was complemented with alternative quantitative measures of the
575 superficial damage induced by liquefaction, such as the Liquefaction Potential Index (LPI) and the Liquefaction
576 Severity Number (LSN).

577 The main conclusion of this paper is that the use of different methodologies for the assessment of liquefaction
578 susceptibility by means of in situ tests is beneficial, particularly if complemented with simple laboratory
579 analyses of grain size distribution and consistency limits. This approach enabled to overcome the limitations
580 of some of the approaches, particularly from SPT and V_s measurements. For the case study of this paper, which
581 involved sensitive loose granular soils, often interbedded with finer soil layers, the laboratory information
582 proved to be of great value to eliminate some discrepancies obtained by the conventional method on SPT data
583 and V_s measurements. However, some discrepancies have not been resolved, evidenced by the LPI and LSN
584 values, since the results from SPT_labFC are still considerably different from CPT results. The presence of
585 many interbedded sand-silt-clay layers was found to compromise an accurate SPT evaluation of the liquefaction
586 potential of the profiles, since the discrete 1-m data points of the SPT are often not representative. In short, the
587 combination of these criteria enabled to identify the areas potentially most affected by liquefaction. Subsequent
588 investigation campaigns are being carried out to refine the database and the results are currently being
589 transferred to geo-statistical modelling software for the microzonation of the pilot site. Complementary
590 information can be found in Viana da Fonseca et al. (2018), Ferreira et al. (2018), Saldanha et al. (2018) and
591 Millen et al. (2019).

592

593

594



LIQUEFACT project (“Assessment and mitigation of liquefaction potential across Europe: a holistic approach to protect structures / infrastructures for improved resilience to earthquake-induced liquefaction disasters”) has received funding from the European Union's Horizon 2020 research and innovation programme under grant agreement No. GAP-700748.

600

601 Acknowledgements are also due to the Portuguese stakeholders of LIQUEFACT, namely Teixeira Duarte, LNEG, ENMC,
602 CMMontijo, CMBenavente, ABLGVFX, BRISA, CENOR, GEOCONTROLE and COBA, as well as to Dr. Luca
603 Minarelli and Dr. Rui Carrilho Gomes. The second and third authors have received funding from FCT (Portuguese
604 Foundation for Science and Technology) in the form of the SFRH/BPD/120470/2016 and SFRH/BD/120035/2016 grants,
605 respectively.

606

607 **NOTATION**

608 a_g – design ground acceleration on type A ground
609 a_{gR} – reference peak ground acceleration on type A ground
610 a_{max} – peak ground acceleration
611 CH – cross-hole test
612 CPTu - piezocone penetrometer test
613 CRR – cyclic resistance ratio
614 CSR – cyclic stress ratio
615 C_σ – overburden coefficient
616 DMT – Flat dilatometer test
617 DWF – Distance Weighting Factor
618 EC8 – Eurocode 8
619 EC8-NA – Eurocode 8, National Annex
620 EILDs – Earthquake Induced Liquefaction Disasters
621 FC – fines content
622 FS_{liq} – factor of safety against liquefaction
623 g – acceleration of gravity
624 h_{liq} – height of liquefiable layer
625 I_C – soil behaviour type index
626 I_D – material index
627 K_{a1} – ageing correction factor
628 K_{a2} – ageing correction factor
629 K_D – horizontal stress index from DMT
630 K_σ – effective overburden stress coefficient
631 LPI – Liquefaction Potential Index
632 LSN – Liquefaction Severity Number
633 MSF – Magnitude Scaling Factor
634 MSF_{max} – upper limit of MSF
635 M_w – moment magnitude
636 $(N_1)_{60cs}$ – normalised equivalent clean sand SPT blow count number
637 p_a – reference atmospheric pressure
638 PI – plasticity index
639 P_L – liquefaction probability
640 q_c – cone tip resistance
641 q_{c1Ncs} – normalised equivalent clean sand CPT cone tip resistance
642 Q_{cn} – normalised cone tip penetration resistance
643 r_d – shear stress reduction coefficient
644 S – soil factor defined in EN 1998-1:2004
645 SASW – Spectral Analysis of Surface Waves test
646 SCPTu – seismic piezocone penetration test
647 SDMT - seismic dilatometer test
648 SI – site investigation point
649 S_{max} – soil factor depending on ground type
650 SPT- standard penetration test

651 SR – seismic refraction test
652 u_2 – pore pressure
653 V_S – shear wave velocity
654 V_{S_AS} – shear wave velocity calculated with Andrus and Stokoe (2000)
655 V_{S_KAE} – shear wave velocity calculated with Kayen et al. (2013)
656 V_{S1} – stress-corrected shear wave velocity
657 V_{S1}^* – upper boundary value of V_{S1}
658 z – depth
659 α – Parameter to calculate r_d
660 β – Parameter to calculate r_d
661 γ_1 – importance factor
662 σ'_v – effective overburden stress
663 σ'_{v0} – initial effective overburden stress
664 τ_{cyc} – cyclic shear stress
665

666 REFERENCES

- 667 American Society of Civil Engineers (2006). Seismic Rehabilitation of Existing Buildings. ASCE/SEI 41-06,
668 Reston, VA.
- 669 American Society of Civil Engineers (2010). Minimum Design Loads for Buildings and Other Structures.
670 ASCE/SEI 7-10, Reston, VA.
- 671 Amoroso, S (2014). Prediction of the shear wave velocity V_s from CPT and DMT at research sites. *Frontiers*
672 *of Structural and Civil Engineering*, 8(1): 83-92, DOI: 10.1007/s11709-013-0234-6, Print ISSN: 2095-
673 2430, Online ISSN: 2095-2449.
- 674 Andrus, RD, NP Mohanan, P Piratheepan, BS Ellis, and TL Holzer (2007). Predicting shear-wave velocity
675 from cone penetration resistance, Proc. 4th Inter. Conf. on Earthq. Geotech. Eng., Thessaloniki, Greece.
- 676 Azevedo, J., Guerreiro, L., Bento, R., Lopes, M. & Proença, J. 2010. Seismic vulnerability of lifelines in the
677 greater Lisbon area. *BullEarthquakeEng* (2010) 8: 157.
- 678 Boncio P., Amoroso S., Vessia G., Francescone M., Nardone M., Monaco P., Famiani D., Di Naccio D.,
679 Mercuri A., Manuel M.R., Galadini F., Milana G. (2018). “Evaluation of liquefaction potential in an
680 intermountain Quaternary lacustrine basin (Fucino basin, central Italy)”, *Bulletin of Earthquake Engineering*,
681 16(1):91-111, Print ISSN 1570-761X, Online ISSN 1573-1456, DOI 10.1007/s10518-017-0201-z,
682 <https://rd.springer.com/article/10.1007/s10518-017-0201-z>
- 683 Boore, DM (2004). Estimating VS(30) (or NEHRP Site Classes) from shallow velocity models (depths < 30m),
684 *Bull. Seismo. Soc. Am.*, 94(2):591–597.
- 685 Boulanger, RW, Idriss, IM (2014). CPT and SPT based liquefaction triggering procedures. Report No.
686 UCD/CGM-14/01. Center for Geotechnical Modeling, University of California, Davis. 134 pp.
- 687 Building Seismic Safety Council (2003). NEHRP Recommended Provisions for Seismic Regulations for New
688 Buildings and Other Structures and Accompanying Commentary and Maps, FEMA 450, Chapter 3, pp. 17–49.
- 689 Cabral J, Moniz C, Batlló J, Figueiredo P, Carvalho J, Matias L, Teves-Costa P, Dias R, Simão N. (2011) The
690 1909 Benavente (Portugal) earthquake: search for the source. *Natural Hazards*. 69: 1211-1227;
691 doi:10.1007/s11069-011-0062-8.
- 692 Caltrans, SDC (2004). Caltrans Seismic Design Criteria, version 1.3. California Department of Transportation,
693 Sacramento, California.
- 694 CEN (2010): Eurocode 8: Design of structures for earthquake resistance.

695 Cubrinovski M, Rhodes A, Ntritsos N, Van Ballegooy S (2017). System response of liquefiable deposits.
696 Proceedings of the 3rd International Conference on Performance-based Design in Earthquake Geotechnical
697 Engineering, Vancouver, 16-19 July 2017.

698 Ferrão C, Bezzeghoud M, Caldeira B, Borges JF (2016). The Seismicity of Portugal and Its Adjacent Atlantic
699 Region from 1300 to 2014: Maximum Observed Intensity (MOI) Map. *Seismological Research Letters* 87(3):
700 743/750. doi: 10.1785/0220150217.

701 Ferreira, C, Viana da Fonseca, A, Saldanha, AS, Ramos, C, Amoroso, S, Minarelli, L (2018) Estimated versus
702 Measured Vs Profiles and Vs30 at a Pilot Site in the Lower Tagus Valley, Portugal. Proceedings of the 16th
703 European Conference on Earthquake Engineering, Thessaloniki, 18-21 June 2018, ID: 10591.

704 GeoLogismiki, 2017. <https://geologismiki.gr/products/cliq/> (accessed in November 2017)

705 Hegazy, Y. A., Mayne, P. W. (1995). Statistical correlations between VS and cone penetration data for different
706 soil types. Proceedings of the International Symposium on Cone Penetration Testing, CPT'95, pp. 173-178.

707 Idriss, I.M. & Boulanger, R.W. 2004. Semi-empirical procedures for evaluating liquefaction potential during
708 earthquakes, in Proceedings, 11th International Conference on Soil Dynamics and Earthquake Engineering,
709 and 3rd International Conference on Earthquake Geotechnical Engineering, D. Doolin et al., eds., Stallion
710 Press, Vol. 1, pp. 32–56

711 Idriss, I.M. & Boulanger, R.W. 2006. Semi-empirical procedures for evaluating liquefaction potential during
712 earth-quakes. *Soil Dyn. and Earthquake Eng.*, 26: 115-130.

713 Idriss, I. M. (1999). An update to the Seed-Idriss simplified procedure for evaluating liquefaction potential.
714 Proc. of the TRB Workshop on New Approaches to Liquefaction, Federal Highway Administration.

715 Idriss, IM, Boulanger, RW (2010). SPT-Based Liquefaction Triggering Procedures. Report No. UCD/CGM-
716 10-02. Center for Geotechnical Modeling, Department of Civil and Environmental Engineering, University of
717 California, Davis. 259 pp.

718 ISO 22476-1:2012 Geotechnical investigation and testing -- Field testing - Part 1: Electrical cone and piezocone
719 penetration test.

720 Iwasaki, T., Tatsuoka, F., Tokida, K. & Yasuda, S. 1978. A practical method for assessing soil liquefaction
721 potential based on case studies at various sites in Japan. Proceedings of the 2nd International Conference on
722 Microzonation. San Francisco, CA, USA, pp. 885–896.

723 Jorge, C. (1993) Zonation of Liquefaction Potential. Application Attempt to the Portuguese Territory. MSc in
724 Sciences in Engineering Geology, New University of Lisbon.

725 Jorge, C., Vieira, A. (1997). Liquefaction Potential Assessment - Application to the Portuguese Territory and
726 to the Town of Setúbal. *Seismic Behaviour of Ground and Geotechnical Structures*, Sêco e Pinto (ed), Balkema:
727 33-43.

728 Kayen, R., Moss, R. E. S., Thompson, E. M., Seed, R. B., Cetin, K. O., Kiureghian, A., Tanaka, Y. and
729 Tokimatsu, K. (2013). Shear-Wave Velocity-Based Probabilistic and Deterministic Assessment of Seismic Soil
730 Liquefaction Potential. *Journal of Geotechnical and Geoenvironmental Engineering*, Vol. 139, N. 3, pp. 407-
731 419. doi:10.1061/(ASCE)GT.1943-5606.0000743

732 Lee, S.H.H. (1992). Analysis of the multicollinearity of regression equations of shear wave velocities, *Soils
733 and Foundations*, 32(1):205–214.

734 Liao, S.S.C. and Whitman, R.V. 1986. A Catalog of Liquefaction and Non-Liquefaction Occurrences during
735 Earthquakes. Research Report. Cambridge: Department of Civil Engineering, Massachusetts Institute of
736 Technology.

737 LIQUEFACT (2017). Project Overview. Available at <http://www.liquefact.eu>. (accessed in November 2017).

738 Marchetti, S., Monaco, P., Totani, G. and Calabrese, M. (2001). The Flat Dilatometer Test (DMT) in Soil
739 Investigations – A Report by the ISSMGE Committee TC16. Proceedings of Int. Conf. on Insitu Measurement
740 of Soil Properties and Case Histories, Bali, 2001, official version reprinted in Flat Dilatometer Testing, Proc.
741 2nd Int. Conf. on the Flat Dilatometer, Washington D.C., April 2-5, 2006, R.A.Failmezger, J.B.Anderson (eds),
742 pp. 7-48.

743 Marchetti, S., Monaco, P., Totani, G. and Marchetti D. (2008). In Situ Tests by Seismic Dilatometer (SDMT).
744 From Research to Practice in Geotechnical Engineering, ASCE, Geotechnical Special Publication, J.E.Laier,
745 D.K.Crapps, M.H.Hussein (eds), Vol. 180, pp. 292-311.

746 Marchetti, S. (1980). "In Situ Tests by Flat Dilatometer". *J. Geotech. Engrg. Div.*, ASCE, 106(GT3), 299-321.

747 Marchetti, S. (2016). Incorporating the Stress History Parameter KD of DMT into the Liquefaction Correlations
748 in Clean Uncemented Sands. *J. Geotech. Geoenviron. Eng.*, 142(2):04015072.

749 Maurer, B., Green, R., Cubrinovski, M., and Bradley, B. 2014. Evaluation of the Liquefaction Potential Index
750 for Assessing Liquefaction Hazard in Christchurch, New Zealand. *Journal of Geotechnical and*
751 *Geoenvironmental Engineering*, ASCE, 140(7). 10.1061/(ASCE)GT.1943-5606.0001117.

752 Mayne, P.W. (2006). In situ test calibrations for evaluating soil parameters. Proc. Characterization and
753 Engineering Properties of Natural Soils II, Singapore.

754 Mayne, P.W. and Rix, GJ (1993). G_{max} - q_c relationships for clays, *Geotechnical Testing Journal*, 16(1):54–60.

755 Millen, M., Ferreira, C., Gerace, A., and Viana da Fonseca, A. (2019). Simplified equivalent soil profiles based
756 on liquefaction performance. 7th International Conference on Earthquake Geotechnical Engineering. Rome,
757 Italy. June 2019.

758 Monaco, P., Tonni, L., Gottardi, G., Marchi, M., Martelli, L., Amoroso and S., Simeoni, L. (2016). "Combined
759 use of SDMT-CPTU results for site characterization and liquefaction analysis of canal levees." *Geotechnical*
760 *and Geophysical Site Characterisation 5 – Lehane, Acosta-Martínez í & Kelly (Eds)*. Australian Geomechanics
761 Society, Sydney, Australia, 615-620, ISBN 978-0-9946261-2-7, [https://australiangeomechanics.org/public-](https://australiangeomechanics.org/public-resources/downloads/#dlISC5)
762 [resources/downloads/#dlISC5](https://australiangeomechanics.org/public-resources/downloads/#dlISC5) Proceedings Monaco, P., Marchetti, S., Totani, G. & Calabrese, M. 2005. Sand
763 liquefiability assessment by Flat Dilatometer Test (DMT). Proc. XVI ICSMGE, Osaka, 4: 2693-2697.

764 Ohta, Y, N Goto (1978). Empirical shear wave velocity equations in terms of characteristic soil indexes, *Earthq.*
765 *Eng. Struct. Dyn.*, 6:167–187.

766 Pirathepan, P (2002). Estimating Shear-Wave Velocity from SPT and CPT Data. Master of Science Thesis,
767 Clemson University.

768 Robertson, P. K., and Wride, C. E. 1997. Cyclic liquefaction and its evaluation based on SPT and CPT.
769 Proceedings, NCEER Workshop on Evaluation of Liquefaction Resistance of Soils.

770 Robertson, P.K. 2012. The James K. Mitchell Lecture: Interpretation of in-situ tests – some insights. Proc. 4th
771 Int. Conf. on Geotechnical and Geophysical Site Characterization, Porto de Galinhas, 1: 3-24.

772 Robertson, P.K. and Wride, C.E. (1998). "Evaluating cyclic liquefaction potential using the cone penetration
773 test". *Canadian Geotech. J.*, 35(3), 442-459.

774 Robertson, PK (2009). Interpretation of cone penetration tests: a unified approach, *Canadian Geotechnical*
775 *Journal*, 46(11):1337–1355.

776 Rodrigues, C., Amoroso, S., Cruz, N., Viana da Fonseca, A. (2016). "Liquefaction assessment CPTu tests in a
777 site in South of Portugal." *Geotechnical and Geophysical Site Characterisation 5 – Lehane, Acosta-Martínez í*
778 *& Kelly (Eds)*. Australian Geomechanics Society, Sydney, Australia, 633-638, ISBN 978-0-9946261-2-7,
779 <https://australiangeomechanics.org/public-resources/downloads/#dlISC5> Proceedings

780 Rollins K.M., Remund T.K., Amoroso, S. (2016). "Evaluation of DMT-Based Liquefaction Triggering Curves
781 Based on Field Case Histories." Geotechnical and Geophysical Site Characterisation 5 – Lehane, Acosta-
782 Martínez í & Kelly (Eds). Australian Geomechanics Society, Sydney, Australia, 639-644, ISBN 978-0-
783 9946261-2-7, https://australiangeomechanics.org/public-resources/downloads/#dIISC5_Proceedings

784 Saldanha, A. S. 2017. Microzonation of liquefaction susceptibility. Application to a case study in the Greater
785 Lisbon area. Master Thesis, Univ. Porto (in Portuguese).

786 Saldanha, A. S., Viana da Fonseca, A., & Ferreira, C. (2018). Microzonation of the liquefaction susceptibility:
787 case study in the lower Tagus valley. *Geotecnia, Journal of the Portuguese Geotechnical Society*, 142, pp. 7-
788 34. doi: 10.24849/j.geot.2018.142.01

789 Seed, H.B. & Idriss, I.M. 1971. Simplified procedure for evaluating soil liquefaction potential. *J. Geotech.*
790 *Engrg. Div., ASCE*, 97(9):1249–1273.

791 Sonmez, H. 2003. Modification of the liquefaction potential index and liquefaction susceptibility mapping for
792 a liquefaction-prone area (Inegol, Turkey), *Environmental Geology*, 44 (2003), pp. 862–871

793 Tonkin & Taylor, 2013. Canterbury earthquakes 2010 and 2011. Land Report as at 29 February 2012.
794 Earthquake Commission (108 pp., [http://www.tonkin.co.nz/canterbury-land-](http://www.tonkin.co.nz/canterbury-land-information/docs/downloads2592013/T&T-Stage-3-Report.pdf)
795 [information/docs/downloads2592013/T&T-Stage-3-Report.pdf](http://www.tonkin.co.nz/canterbury-land-information/docs/downloads2592013/T&T-Stage-3-Report.pdf)).

796 Tsai, P., Lee, D., Kung, G.T. & Juang, C.H. 2009. Simplified DMT-based methods for evaluating liquefaction
797 resistance of soils. *Engineering Geology*, 103: 13-22.

798 Viana da Fonseca, A, Ferreira, C, Ramos, C (2017). D2.1 – Part 2: Report on ground characterization of the
799 four areas selected as testing sites by using novel technique and advanced methodologies to perform in situ and
800 laboratory tests – Lisbon Area in Portugal. Deliverable D2.1 of the European H2020 LIQUEFACT research
801 project. January 2017.

802 Viana da Fonseca, A, Ferreira, C, Saldanha AS, Ramos, C, Rodrigues, C (2018). Comparative analysis of
803 liquefaction susceptibility assessment by CPTu and SPT tests. *Cone Penetration Testing 2018, Proceedings of the*
804 *4th International Symposium on Cone Penetration Testing (CPT'18)*, Hicks, Pisanò & Peuchen (Eds.), pp. 669–675. CRC
805 Press, Delft, The Netherlands.

806 Vilanova, S, Fonseca, J (2007). Probabilistic seismic-hazard assessment for Portugal, *Bull. Seismol. Soc. Am.*
807 97, no. 5, 1702–1717.

808 Wair BR, DeJong JT, Shantz T (2012) Guidelines for Estimation of Shear Wave Velocity Profiles. PEER
809 Report 2012/08. Pacific Earthquake Engineering Research Center.

810 Wood, CM, McGann, CR, Cox, BR, Green, R, Wotherspoon, L, Bradley, BA, Cubrinovski, M (2017). A
811 comparison of CPT-Vs correlations using a liquefaction case history database from the 2010-2011 Canterbury
812 Earthquake Sequence. *Proceedings of the 3rd International Conference on Performance-based Design in*
813 *Earthquake Geotechnical Engineering (PBD-III)*, Vancouver, BC, Canada, July 16-19, 2017.

814 Wotherspoon, LM, Orense, RP, Green, RA, Bradley, BA, Cox, BR, Wood, CM, 2015. Assessment of
815 liquefaction evaluation procedures and severity index frameworks at Christchurch strong motion stations, *Soil*
816 *Dynamics and Earthquake Engineering*, Volume 79, Part B, 2015, pp. 335-346, ISSN 0267-
817 7261, <https://doi.org/10.1016/j.soildyn.2015.03.022>.

818 Youd, T. L., Idriss, I. M., Andrus, R. D., Arango, I., Castro, G., Christian, J. T., ...& Ishihara, K. 2001.
819 Liquefaction resistance of soils: summary report from the 1996 NCEER and 1998 NCEER/NSF workshops on
820 evaluation of liquefaction resistance of soils. *Journal of Geotechnical and Geoenvironmental Engineering*,
821 127(10), 817-833.

- 822 Youd, T.L. and Idriss, I.M. (2001). "Liquefaction Resistance of Soils: Summary Report from the 1996 NCEER
823 and 1998 NCEER/NSF Workshops on Evaluation of Liquefaction Resistance of Soils". J. Geotech.
824 Geoenviron. Eng., ASCE, 127(4), 297-313.
- 825 Zhang, G., Robertson, P.K. & Brachman, R.W. 2002. Estimating liquefaction-induced ground settlements from
826 CPT for level ground. Canadian Geotechnical Journal, 39(5), pp.1168–1180.